Vertebrates show coordinated elevated expression of mitochondrial and nuclear genes after birth

Hadar Medini and Dan Mishmar

Genome Res. 2025 35: 459-474 originally published online March 4, 2025
Access the most recent version at doi:10.1101/gr.279700.124

Research

Vertebrates show coordinated elevated expression of mitochondrial and nuclear genes after birth

Hadar Medini and Dan Mishmar

Department of Life Sciences, Ben-Gurion University of the Negev, Beer-Sheva 8410501, Israel

Interactions between mitochondrial and nuclear factors are essential to life. Nevertheless, the importance of coordinated regulation of mitochondrial–nuclear gene expression (CMNGE) to changing physiological conditions is poorly understood and is limited to certain tissues and organisms. We hypothesized that CMNGE is important for development across vertebrates and, hence, should be conserved. As a first step, we analyzed more than 1400 RNA-seq experiments performed during prenatal development, in neonates, and in adults across vertebrate evolution. We find conserved sharp elevation of CMNGE after birth, including oxidative phosphorylation (OXPHOS) and mitochondrial ribosome genes, in the heart, hindbrain, forebrain, and kidney across mammals, as well as in *Gallus gallus* and in the lizard *Anolis carolinensis*. This is accompanied by elevated expression of TCA cycle enzymes and reduction in hypoxia response genes, suggesting a conserved cross-tissue metabolic switch after birth / hatching. Analysis of about 70 known regulators of mitochondrial gene expression reveals consistently elevated expression of *PPARGC1A* (also known as *Pgc-1alpha*) and *CEBPB* after birth / hatching across organisms and tissues, thus highlighting them as candidate regulators of CMNGE upon transition to the neonate. Analyses of *Danio rerio*, *Xenopus tropicalis*, *Caenorhabditis elegans*, and *Drosophila melanogaster* reveal elevated CMNGE prior to hatching in *X. tropicalis* and in *D. melanogaster*, which is associated with the emergence of muscle activity. Lack of such an ancient pattern in mammals and in chickens suggests that it was lost during radiation of terrestrial vertebrates. Taken together, our results suggest that regulated CMNGE after birth reflects an essential metabolic switch that is under strong selective constraints.

[Supplemental material is available for this article.]

Mitochondria are pivotal to cellular metabolism across all eukaryotes. In animal cells, unlike most cellular pathways, the mitochondrial genetic system is the only system with factors encoded by two genomes, in two cellular compartments: the nucleus and the mitochondria. It has been shown that genes encoded by the two genomes that participate in the same pathway, such as the energy-producing oxidative phosphorylation system (OXPHOS), have coevolved and that interference with such coevolution affects fitness (Gershoni et al. 2009; Meiklejohn et al. 2013; Bar-Yaacov et al. 2015; Barreto et al. 2018; Hill et al. 2019; Moran et al. 2024). We and others previously found that coordination of gene expression between the mitochondrial (mtDNA) and nuclear genomes, especially in the OXPHOS system, is common across most healthy human tissues (Barshad et al. 2018), a variety of cancer samples (Reznik et al. 2017), and in certain cell types (Medini et al. 2021a), yet is compromised in several disease conditions, including COVID19, Alzheimer's disease, and several cancer types (Medini et al. 2021b; Papier et al. 2022). It is thus reasonable to assume that coordinated mitonuclear gene expression (CMNGE) is important, will respond to changing environments, and will change upon alteration of physiological conditions, such as the changes that occur during prenatal development and in the transition to the neonate (Sharma et al. 2014).

Indeed, mitochondrial activity, morphology, number, and regulation of replication and transcription are critical for cell differentiation and development (Folmes et al. 2011; Hom et al. 2011; Wellen and Thompson 2012; Medini et al. 2020). Specifically, knockout of mitochondrial regulatory proteins such as mtDNA polymerase gamma (*Polg*) (Hance et al. 2005) and mtDNA transcription factor A (*Tfam*) (Larsson et al. 1998) resulted in developmental arrest between embryonic days 7.5 and 8.5 (upon *Polg* knockout) and lethality on day 10.5 of mouse embryos (upon *Tfam* knockout). In addition, knockout of mitochondrial RNA polymerase (*rpom-1*) resulted in decreased brood size and impaired ova development in the worm *Caenorhabditis elegans* (Charmpilas and Tavernarakis 2020). Second, knockout of *Nrf1*, a key regulator of nuclear DNA–encoded OXPHOS gene expression, led to mouse embryonic lethality (Chan et al. 1998). Third, knockout of another regulator of OXPHOS genes expression, *Nfe2l2* (also known as *Nrf2*), led to a reduction in the levels of NADPH and the NADPH/NADP+ ratio in embryonic mouse fibroblasts (Singh et al. 2013), and ATP levels were significantly reduced upon *NFE2L2* (also known as *NRF2*) knockdown in human cancer cell lines (Kim et al. 2011). Both *NRF1* and *NRF2* are involved in mitochondrial biogenesis via the regulation of peroxisome proliferator–activated receptor-gamma coactivator-1alpha (*PPARGC1A*), an OXPHOS master regulator (Gureev et al. 2019; Deng et al. 2020). Accordingly, targeted deactivation of *Ppargc1a* (also known as *Pgc-1alpha*) as well as a transcription factor from the same family, *Ppargc1b*, also known as *Pgc-1beta* (*PGC-1*$\alpha\beta^{-/-}$) in the mouse heart led to reduced growth, late fetal arrest in mitochondrial biogenesis (at E16.5 and E17.5), and 70% lethality of mice within 24 h after birth (Lai et al. 2008). Fourth, dysfunctional mitochondria in the embryonic mouse and human patients' hearts led to severe cardiomyopathy and either embryonic or neonatal lethality (Zhao et al. 2019). Taken together, transcriptional regulation of mitochondrial

Corresponding author: dmishmar@bgu.ac.il
Article published online before print. Article, supplemental material, and publication date are at https://www.genome.org/cgi/doi/10.1101/gr.279700.124.

genes in both the nucleus and the mtDNA is pivotal for the developing embryo and for the transition to the neonate.

Studies in model organisms support the occurrence of a metabolic shift after birth in certain tissues. Quantification of lactic acid in rat livers revealed that glycolysis is decreased after birth (Burch et al. 1963). Consistent with this finding, the human postnatal liver and heart collected 6 and 36 weeks after birth displayed an increase in mitochondrial content and respiratory chain activities compared with fetal samples collected after 11–17 weeks of gestation (Minai et al. 2008). Finally, an increased level of the mitochondrial electron carrier cytochrome c was observed in newborn human and rat livers compared with fetal samples (Krizova et al. 2021).

These pieces of evidence led us to hypothesize that there is a regulated increase in OXPHOS function after birth, which is conserved in evolution. Our analysis relies on the notion that genes belonging to the same pathway, including OXPHOS, tend to be coregulated (van Waveren and Moraes 2008; McShane et al. 2024). To test this hypothesis, we interrogated N = 1482 RNA-seq experiments from samples collected during embryo and fetal development as well as after birth from a variety of metazoans in several different tissues (Fig. 1).

Results

Postnatal mtDNA gene expression is generally elevated across evolution

To assess the dynamics of mitochondrial transcript regulation during metazoan development, we have analyzed publicly available bulk RNA-seq data from six mammals—*Homo sapiens*, human; *Macaca mulatta*, rhesus monkey; *Mus musculus*, mouse; *Rattus norvegicus*, rat; and *Oryctolagus cuniculus*, rabbit—and from *Gallus gallus* (chicken). The data were generated from seven tissues collected during prenatal and postnatal development (Data set I; Methods) (Table 1; Cardoso-Moreira et al. 2019; Chen et al. 2022). This analysis was augmented by analysis of RNA-seq from samples collected from *Sus scroffa* (pig) liver during prenatal stages and from the neonate (Data set II). To identify the specific time frame in which potential transition in gene expression occurred, the data were analyzed in sliding windows of available developmental stages, while testing a variable number of consecutive stages (e.g., windows containing either two, four, or six of the tested developmental stages; see Methods). Window sizes w = 4 and w = 6 showed similar trends (Supplemental Figs. S1–S6); however, given the limited number of time points in chicken samples (mostly n = 9), we reasoned that using w = 6 would reduce resolution and potentially mask key shifts in gene expression. Window w = 2, on the other hand, increased the noise. Therefore, for consistency, w = 4 was chosen in the analyses across species, offering sufficient resolution in all tested organisms. For each time point, we computed the average fold-change (FC) of mtDNA genes' expression and identified the time points with the highest mean FC. Our findings revealed significantly elevated mtDNA gene expression, which was observed in postnatal samples from five out of seven tissues across all tested species, with one exception: reduction in mtDNA gene expression in chicken liver after hatching (see below) (Fig. 2A,B; Supplemental Fig. S7). Specifically, we found elevated mtDNA genes' expression right after or at 1–2 weeks after birth/hatching in the heart in six of

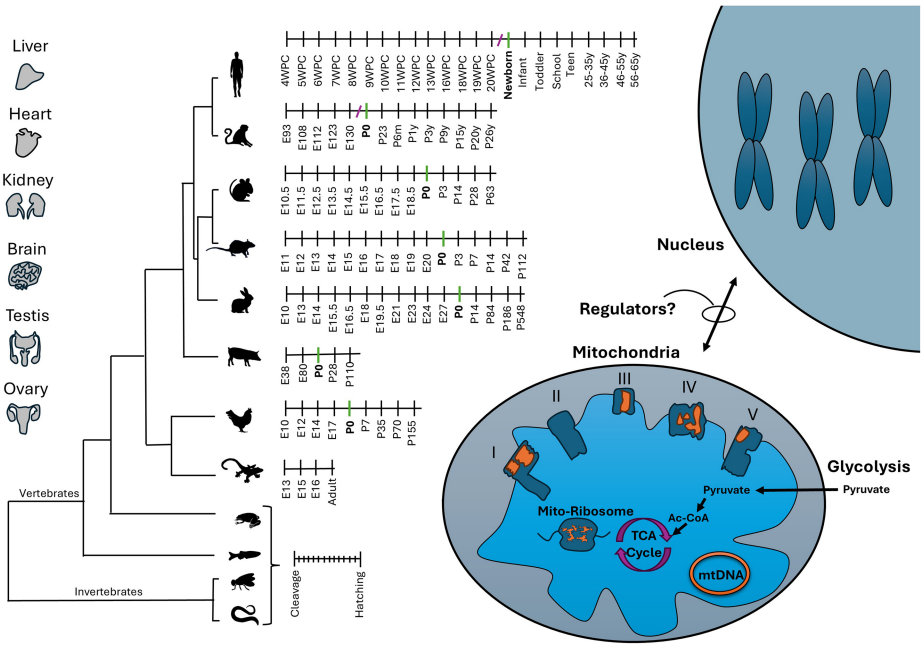

Figure 1. Roadmap to assessment of mitonuclear gene expression (RNA-seq) during the course of development and evolution. Tissues analyzed (indicated) were collected from six mammals (*Homo sapiens*, *Macaca mulatta*, *Mus musculus*, *Rattus norvegicus*, *Oryctolagus cuniculus*), as well as from *Gallus gallus* (chicken), during development. The developmental stages are indicated per organism, and P0 (birth/hatching) is highlighted for mammals and birds. Missing stages (owing to lack of samples) are indicated by "/." To avoid sample size issues, gene expression in *Anolis carolinensis* (brain, heart, kidney, liver) was compared between a group of embryonic versus adult samples (e.g., not divided into further stages). Analysis of additional nonmammalian vertebrates, for example, *Xenopus tropicalis* (tropical frog) and *Danio rerio* (zebrafish), as well as two invertebrates, for example, *Drosophila melanogaster* and *Caenorhabditis elegans*, was limited to the prenatal stages. mtDNA and nuclear DNA–encoded subunits of OXPHOS complexes I, III, IV, and V are indicated in orange and dark blue, respectively. Additional selected metabolic pathways are indicated, including the mitochondrial ribosome (mito-ribosome), tricarboxylic acid cycle (TCA), and glycolysis. The lack of knowledge of regulators of mitonuclear gene expression is indicated.

Table 1. Resources for RNA-seq data per tissue and organism

Data set	Organism(s) analyzed	Tissue	Include P0 (neonate right after birth)	Resource
I	Human (N = 297), rhesus (N = 168), mouse (N = 316), rabbit (N = 315), rat (N = 350), chicken (N = 215)	Heart, cerebrum/hindbrain, cerebellum/forebrain, kidney, liver, testis, ovary	Yes	Cardoso-Moreira et al. (2019)
II	Pig (N = 30)	Liver	Yes	Chen et al. (2022)
III	Chicken (N = 9)	Liver	No	Xu et al. (2019)
IV	Mouse (N = 19)	Heart	No	Matkovich et al. (2014)
V	*Anolis carolinensis* (N = 78)	Brain, heart, kidney, liver	No	Marin et al. (2017)
VI	*Xenopus tropicalis* (N = 40)	Whole embryo	No (only prenatal)	Mitros et al. (2019)
VII	*Danio rerio* (zebrafish) (N = 56), *Drosophila melanogaster* (N = 77) and *Caenorhabditis elegans* (N = 81)	Whole embryo	No (only prenatal)	Levin et al. (2016)

six of the tested organisms, in the forebrain/cerebrum in five of six organisms (human, rat, rabbit, mouse, and rhesus monkey), in hindbrain/cerebellum samples in six of six organisms, in kidney samples in four of six organisms (human, mouse, chicken, and rhesus), in liver samples in five of seven organisms (human, rat, mouse, rabbit, and pig—the only tissue tested in the latter), and in testes only in rhesus monkey (Table 2). Further support for the elevation of mtDNA gene expression after birth came from the analysis of other additional RNA-seq data sets collected from postnatal mouse heart samples compared with embryonic samples (Data set IV, embryos collected from gestational day 13.5 vs. samples collected 6 weeks after birth) (Supplemental Fig. S8; Matkovich et al. 2014). All these results reflect a conserved elevation of mtDNA gene expression across tissues, implying a conserved regulatory mechanism.

While considering the liver, we noticed that, unlike mammals, chicken liver displayed a reduction in mtDNA gene expression during the first week after hatching. This finding gained support from the analysis of an additional data set (Data set III), which includes chicken liver samples from embryonic day 13, compared with samples collected 5 weeks after hatching (Supplemental Fig. S9; Xu et al. 2019). We interpret the divergent mtDNA gene expression pattern in the chicken liver compared with the mammalian liver as likely associating with the accumulation of fat in the chick liver but not in mammals, thus offering a different carbon source for OXPHOS activity in chicken liver after hatching (see Discussion).

Our analysis so far focused mostly on mammals with one nonmammalian vertebrate: the chicken. To assess whether our observed elevated mtDNA gene expression after birth is shared across other vertebrates, we sought to extend our analysis to other additional nonmammalian vertebrates. Accordingly, analysis of RNA-seq experiments generated from 48 embryonic samples from the lizard *Anolis carolinensis* (collected from developmental stages 15–16) compared with 30 adult samples from four organs (brain, heart, kidney, liver; Data set V) (Marin et al. 2017) revealed elevated mtDNA genes expression in the adult heart, brain, and kidney. The *A. carolinensis* liver did not show any consistent pattern (Fig. 2B; Supplemental Fig. S10). This finding suggests that elevated mtDNA gene expression after birth is conserved across mammalian and terrestrial nonmammalian vertebrates.

Expression of postnatal nuclear DNA–encoded OXPHOS gene is elevated across evolution

As mtDNA-encoded proteins interact with nuclear DNA–encoded subunits of the OXPHOS system, we sought to assess the expression pattern of the latter during fetal development and after birth. Our findings indicate that the same tissues that showed elevated mtDNA gene expression also showed clear elevation of nuclear DNA–encoded OXPHOS gene expression in Data sets I, II, and IV (Table 2; Fig. 3A,B; Supplemental Figs. S11, S12). It is worth noting that we used the sliding windows approach as in the mtDNA analyses (Supplemental Figs. S13–S18). This finding supports the hypothesis that the elevation of OXPHOS genes' expression after birth/hatching is coordinated between the mtDNA and the nucleus (mitonuclear). To quantify the level of CMNGE in each of the tested organisms and tissues, we calculated the number of significantly altered expression of mtDNA genes and nuclear DNA–encoded OXPHOS genes and divided them by the number of genes with available expression information (in each available data set, separately). This analysis revealed that the heart displayed high coordination level in all organisms analyzed (average 0.8, SD 0.08) (Table 2; Fig. 3B; Supplemental Table S1). Moreover, the organisms that displayed change in mtDNA gene expression during the first weeks after birth/hatching also displayed CMNGE in the same days, including chicken liver that showed coordinated downregulation in OXPHOS genes (level of coordination = −0.6, e.g., downregulation; Data set I) (Table 2; Fig. 3B; Supplemental Table S1; Supplemental Figs. S11, S19). An exception was the chicken hindbrain/cerebellum, which displayed elevated mtDNA gene expression between P0 and P7 days after birth yet decreased OXPHOS nuclear genes' expression during the same days (level of coordination = −0.19; e.g., downregulation). This observation awaits confirmation once additional RNA-seq data sets become available from chicken samples collected from the hindbrain during development. In the *A. carolinensis* (hereon lizard) heart, and to a lower extent in the kidney, we observed a tendency toward an elevated expression of structural nuclear DNA–encoded OXPHOS genes (Supplemental Fig. S20). The lizard brain did not show a consistently elevated OXPHOS gene expression in the adult. These results suggest that CMNGE is observed in the lizard heart and in the kidney. Finally, it is worth noting that while considering mammals and the chicken, structural subunits of the OXPHOS showed

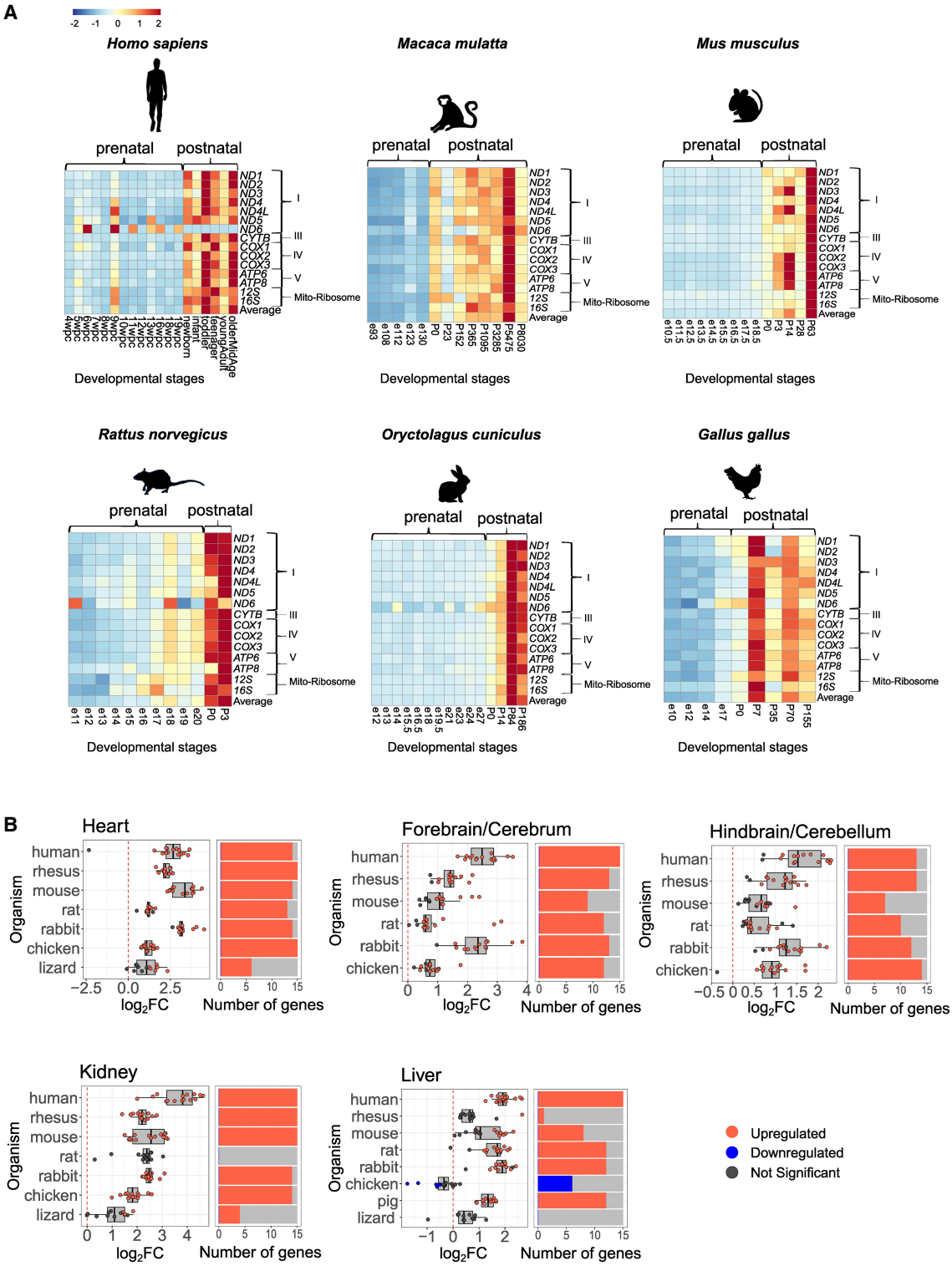

Figure 2. mtDNA gene expression is elevated in postnatal vertebrate samples. (*A*) Heatmaps representing mtDNA gene expression in heart from five mammals and in the chicken. Color bar indicates the scaled expression. Red scale indicates elevated expression; blue scale, reduced expression. The *x*-axis indicates prenatal and postnatal stages of sample collection; *y*-axis, mtDNA genes and their OXPHOS complex assignments. (*B*, *left*) Box plots indicating the $\log_2$FC of mtDNA genes. The *x*-axis indicates Log_2FC; *y*-axis, the tested organisms: *H. sapiens*, human; *M. mulatta*, rhesus; *M. musculus*, mouse; *R. norvegicus*, rat; *O. cuniculus*, rabbit; *G. gallus*, chicken; *Sus scroffa*, pig; and *A. carolinensis*, lizard. Color bar: blue dots indicate downregulation ($\log_2\text{FC} < -0.2$, *P*-value < 0.05); red dots, upregulation ($\log_2\text{FC} > 0.2$, *P*-value < 0.05); and gray dots, nonsignificant. Dashed vertical red line displays the value of zero $\log_2$FC on *x*-axis. (*Right*) Bar plots representing the number of significant (indicated in red or blue) and nonsignificant (NS) mtDNA genes expression (colored in gray). Blue indicates statistically significant genes with decreased expression between the time points ($P < 0.05$); red, number of genes with significantly increased expression. The *x*-axis indicates *n*umber of genes; *y*-axis, tested organisms.

Table 2. The developmental time point presenting the highest fold-change of either upregulation or downregulation of mtDNA gene expression in samples from Data sets I and II

	Before P0	Right after birth/hatching	First week/s after birth	Late change
Heart	—	Human (0.87), mouse (0.88), rat (0.72), rhesus (0.86), chicken (0.66)	Rabbit (0.83)	—
Forebrain/ cerebrum	Chicken (0.35)	Human (0.72), rat (0.06), rhesus (0.65)	Mouse (0.37), rabbit (0.59)	—
Hindbrain/ Cerebellum	—	Human (0.62), rat (0.19), rhesus (0.41), chicken (–0.19)	Mouse (0.69), rabbit (0.52)	—
Kidney		Human (0.78), mouse (0.84), rhesus (0.88)	Chicken (0.16), rat (0)	Rabbit (0.79)
Liver		Human (0.23), pig (0.8), rat (0.03)	Chicken[a] (–0.6), mouse (0.67), rabbit (0.27)	Rhesus (0)
Testis	Human, rabbit, rat[a]	Chicken,[a] rhesus		Mouse[a]
Ovary	Chicken,[a] rabbit, rat[a]			

[a]Downregulation; the rest were upregulated. Numbers in parentheses indicate the level of coordination of nuclear DNA–encoded OXPHOS genes and mtDNA-encoded genes as explained in the Methods.

a sharper elevation in gene expression after birth than did OXPHOS assembly subunits (Fig. 3; Supplemental Figs. S21–S27). This suggests that for OXPHOS, elevated CMNGE after birth/hatching is more coordinated among the inherent structural members of the OXPHOS system.

Altered mitonuclear OXPHOS gene expression after birth is part of a wider metabolic switch

Because elevation in OXPHOS function after birth could be part of a general functional mitochondrial shift, we asked whether gene expression of any other mitochondrial pathways is altered after birth. Therefore, we compared gene expression of the following mitochondrial-related pathways before and after birth: the mitochondrial ribosome, the tricarboxylic acid cycle (TCA), formation, and scavenging of reactive oxygen species (ROS), in addition to glycolysis.

First, the mitochondrial ribosome, which like the OXPHOS incorporates factors encoded by the nuclear and mitochondrial genomes, showed coordinated mitonuclear expression changes in heart of all organisms, except for the lizard (average 0.62, SD 0.24) (Supplemental Fig. S28; Supplemental Table S1), and in the kidney of humans, the rhesus monkey, and rabbit (levels of coordination = 0.64, 0.87, and 0.65, respectively). In addition, we observed strong CMNGE in the pig liver (Data set II, level of coordination = 0.78). The same trend, although to a lower extent, was observed in the mouse (Data set I, level of coordination = 0.28) but not in the liver of other tested mammals. In contrast, we observed a reduction of gene expression in the chicken liver as in OXPHOS genes (level of coordination = –0.52; e.g., downregulation). Finally, we found significantly decreased expression of the ribosomal genes in the cerebellum only in the chicken, similar to the OXPHOS genes (level of coordination = –0.5; e.g., downregulation) (Supplemental Fig. S28). These results suggest that the mitochondrial ribosomal genes undergo a similar expression change after birth as in OXPHOS, especially in the heart.

Second, we identified sharply elevated expression of genes related to the TCA cycle mainly in the heart and kidney after birth/hatching, as well as in several organisms in the rest of the tested tissues (Supplemental Fig. S29). Similar to the OXPHOS genes and the mitochondrial ribosome, the chicken liver displayed reduced TCA cycle genes' expression. Taken together, these results support a conserved overall functional metabolic shift in the mitochondria after birth or hatching across tissues and across the evolution of vertebrates.

Our analysis of genes involved in glycolysis did not reveal any consistent overall expression pattern change while jointly considering a pathway in the comparison of prenatal and postnatal samples (Supplemental Fig. S30A). Nevertheless, lactate dehydrogenase (*LDH*), a key glycolysis enzyme, showed an interesting pattern: *LDH* has two subunits: *LDHA* and *LDHB*; the first is known to be upregulated mostly in glycolytic conditions, whereas *LDHB* is commonly upregulated in conditions that require OXPHOS (Read et al. 2001; Porporato et al. 2011). Although *LDHA* did not show any significantly conserved expression pattern across all tested tissues, it decreased in the heart after birth in four of six tested species (Supplemental Fig. S30B,C). *LDHB* was significantly upregulated in several tissues that displayed mitonuclear upregulation across species: the forebrain and hindbrain in three of six organisms, the kidney in four or six organisms, and the heart in five of six of the tested organisms (Supplemental Fig. S30B). It is worth noting that the expression of enzymes and regulators of the ROS scavenging pathway was not significantly altered in all tested mammals and in the chicken (Supplemental Fig. S31). These results suggest that by and large, OXPHOS likely replaced glycolysis as the dominant ATP source after birth at least in the mentioned tissues.

Nevertheless, the liver displayed significantly reduced *LDHB* expression after birth/hatching in four of seven species (human, rhesus, mouse, and chicken) (Supplemental Fig. S30B,C). Because the liver is known to have special metabolic activities, including gluconeogenesis, we asked whether the expression pattern we observed for OXPHOS and *LDHB* is also associated with similar expression changes of the key enzyme of this pathway, phosphoenolpyruvate carboxykinase (*PCK2,* also known as *PEPCK*) (Hanson and Reshef 1997). *PEPCK* (*PCK1*; the cytosolic form) also has a mitochondrial isoform, *PCK2*. Although *PCK2* did not show any clear expression pattern change after birth/hatching, *PCK1* was generally upregulated in all mammalian tissues

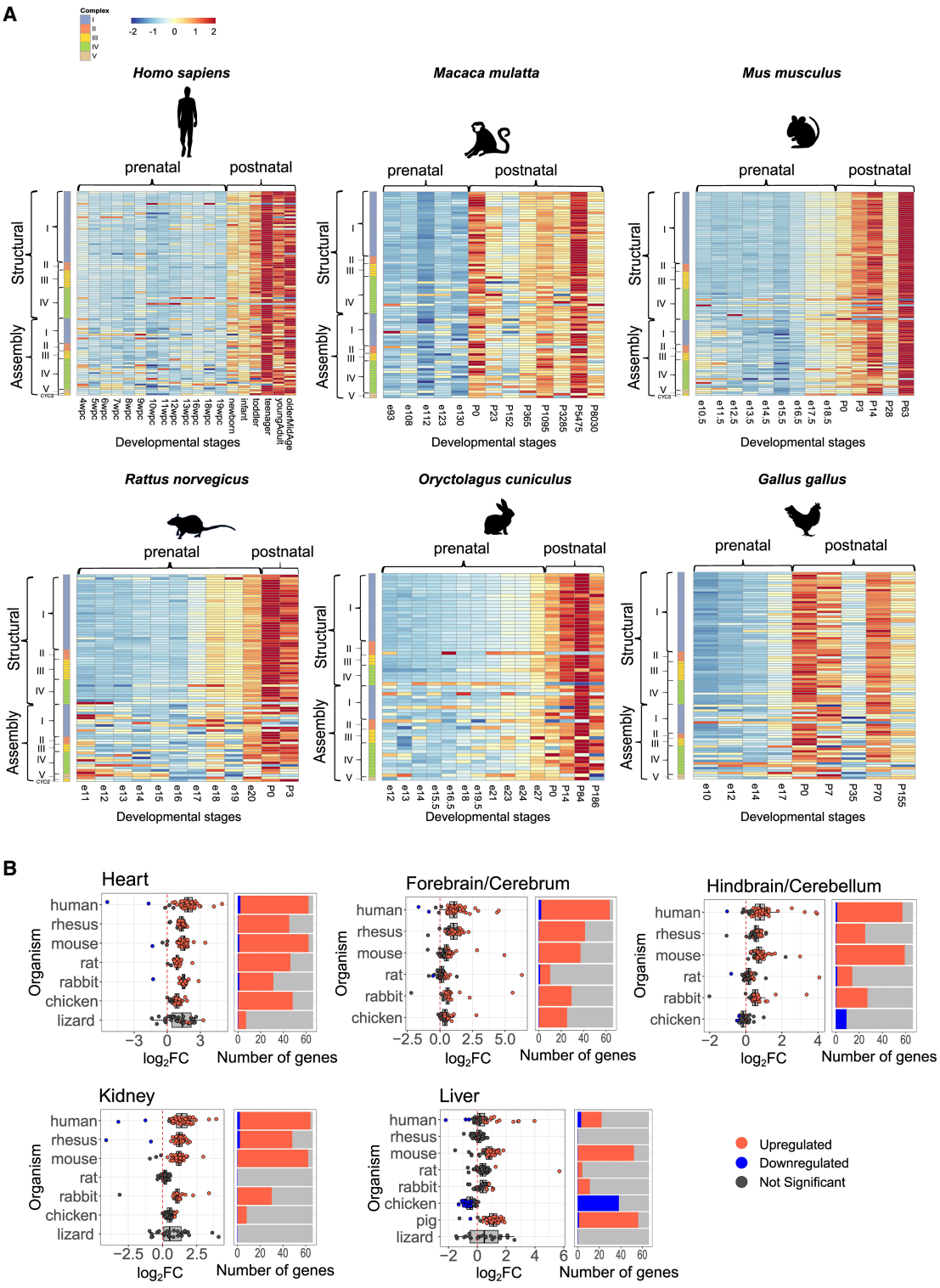

Figure 3. Nuclear DNA–encoded OXPHOS genes expression is elevated after birth/hatching across vertebrates. (*A*) Heatmaps representing expression of nuclear DNA–encoded OXPHOS gene in the heart from five mammals and in birds. Color bar: red scale indicates elevated expression; blue scale, reduced expression. *Above* each panel are the labels of the prenatal and postnatal samples. The *x*-axis indicates developmental stages; *y*-axis, nuclear DNA–encoded genes, divided according to OXPHOS complexes, structural and assembly genes, and Cytochrome C (*CYCS*). (*B*, *left*) Box plots indicating the log_2FC of nuclear DNA–encoded structural subunits of the OXPHOS. The *x*-axis indicates Log_2FC; *y*-axis, the tested organisms. Color bar: blue dots indicate down-regulation ($log_2FC < -0.2$, *P*-value < 0.05); red dots, upregulation ($log_2FC > 0.2$, *P*-value < 0.05); and gray dots, nonsignificant. Dashed vertical red line displays the value of zero log_2FC on the *x*-axis. (*Right*) Bar plots representing the number of significant (indicated in red or blue) and nonsignificant (NS) nuclear OXPHOS genes expression (colored in gray). Blue indicates statistically significant genes with decreased expression between the time points ($P < 0.05$); red, number of genes with significantly increased expression. The *x*-axis indicates number of genes; *y*-axis, organisms.

and in the chicken heart. The expression of *PCK1* was significantly elevated in the liver of four mammals (human, mouse, rat, and pig), yet did not significantly change in the chicken or in the chicken kidney after hatching, the main tissues in which gluconeogenesis takes place (Supplemental Fig. S32; Supplemental Table S1). In summary, the generally elevated expression of *PCK1* in the mammalian liver and the lack of change in *PCK1* in the chicken liver, along with only partial elevation of OXPHOS in this tissue in mammals and reduction of *LDHB* expression in mammals, may reflect a unique involvement of the OXPHOS in liver metabolism during evolution.

The lizard *A. carolinensis* did not show any consistent pattern in these pathways when comparing embryo to adult samples (Supplemental Figs. S33–S37; Supplemental Table S1). This suggests that although the lizard did show a trend toward elevated OXPHOS gene expression in postnatal periods, more detailed expression analysis in this species after hatching may shed light on the involvement of other additional metabolic pathways.

Taken together, the CMNGE-coordinated upregulation of mitonuclear gene expression (e.g., OXPHOS and the mitochondrial ribosome) is a widespread phenomenon across somatic tissues, is highly conserved among mammals and chicken, and is accompanied by significant elevation of TCA cycle enzymes. This supports an overall change in mitochondrial metabolism after birth/hatching that is regulated already at the transcript level.

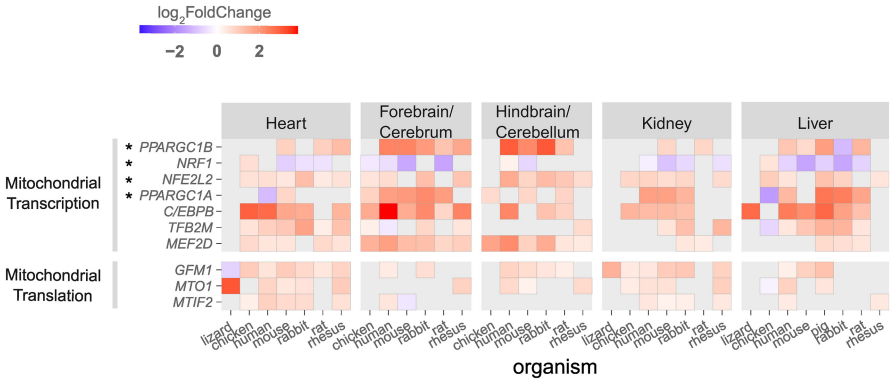

Figure 4. Expression of regulatory factors that modulate mitochondrial biogenesis associates with mitonuclear expression shift after birth/hatching across vertebrates. Heatmap presenting $\log_2$FC values of regulatory factors and genes related to mitochondrial biogenesis that displayed significant change in at least four tissues within any organism and in at least five organisms within any tissue (*P*-value < 0.05). Color bar indicates the $\log_2$FC. The *x*-axis indicates organisms divided by tissues; *y*-axis, genes. Only $\log_2$FC > 0.2 and $\log_2$FC < −0.2 are shown. (*) Genes related to mitochondrial biogenesis.

The elevated expression and CMNGE after birth associates with altered expression of regulatory factors that modulate mitochondrial biogenesis

The discovery of elevated CMNGE in vertebrates during the transition to the neonate suggests an underlying regulatory mechanism. Accordingly, it is conceivable that certain regulators of mitonuclear transcripts modulate CMNGE elevation after birth. To identify such factors, we tested for two categories (transcription and post-transcription), while highlighting transcription factors involved in mitochondrial biogenesis. To this end, we analyzed bulk RNA-seq samples from Data sets I and II, including six mammals and chicken, for the expression pattern of about 70 known mitochondrial regulatory factors, including mitochondrial transcription, post-transcriptional activities, and biogenesis-related genes (Fig. 4; Supplemental Tables S1, S2; Supplemental Figs. S38–S40). Specifically, we compared the expression of these genes in tissue samples that preceded the time point at which the OXPHOS expression transition occurred to the samples right after the transition in each organism.

As we expected that only a few factors would be involved in the elevated CMNGE in the neonate, we counted for each factor the number of organisms and corresponding tissues that displayed significant value in the tested factors. Specifically, we considered factors as candidates if they consistently displayed significantly altered expression in the transition to neonatal life in at least four tissues within any organism and at least five organisms within any tissue (Fig. 4).

First, our analysis highlighted PPARG coactivator 1 alpha (*PPARGC1A*, PGC-1alpha), as a regulatory factor whose expression pattern best resembled the pattern of OXPHOS genes across organisms and tissues. *PPARGC1A* is regulated by environmental stimuli and is considered central in regulating mitochondrial biogenesis (Puigserver et al. 1998). Similar to mitonuclear OXPHOS genes, *PPARGC1A* was significantly upregulated in the liver of four of eight organisms—human ($\log_2$FC = 1.39), pig ($\log_2$FC = 2.64), rabbit ($\log_2$FC = 2.5), and rat ($\log_2$FC = 1.77)—whereas it was downregulated in the chicken liver ($\log_2$FC = −1.65). The elevated expression of *PPARGC1A* was also apparent in the forebrain/cerebrum (five of six organisms), hindbrain/cerebellum (three of six organisms), and kidney (three of seven), yet was not clearly evident in the heart (only in the mouse) (Fig. 4; Supplemental Fig. S38). This result supports the association of elevated CMNGE after birth with altered regulation of mitochondrial biogenesis in most tested tissues.

Second, NFE2L2 (also known as NRF2), a transcription factor that responds to oxidative stress and is involved in the regulation of mitochondrial biogenesis via regulation of *PPARGC1A* (Gureev et al. 2019; Deng et al. 2020), was significantly upregulated in the following tissues and organisms (Fig. 4; Supplemental Fig. S38; Supplemental Table S1): in the heart (all organisms, except for the lizard), in forebrain/cerebrum (four of six organisms), in hindbrain/cerebellum (five of six), in the kidney of five of seven organisms, and in liver of five of eight organisms. Unlike *PPARGC1A*, *NFE2L2* expression was elevated in chicken liver.

Third, CCAAT enhancer binding protein beta (*CEBPB*) was significantly upregulated in the heart of five of seven organisms, in the forebrain/cerebrum of all organisms, in the hindbrain/cerebellum of three of six organisms, in the kidney of four of seven organisms, and in the liver of six of eight organisms (Fig. 4; Supplemental Fig. S38). Previous analysis of ChIP-seq experiments from the ENCODE consortium revealed that *CEBPB* binds upstream regulatory elements of OXPHOS genes more than expected by chance (Blumberg et al. 2014). This is the only transcription factor in the current analysis that was experimentally shown to both regulate nuclear gene transcription, bind the mtDNA in vivo, and localize to the mitochondria in human cells (Blumberg et al. 2014). CEBPB is a transcription factor involved in inflammation, metabolism, and differentiation as well as in fatty acid metabolism in collaboration with *PPARGC1A*

(Takagi et al. 2022). Therefore, CEBPB is an attractive candidate to regulate the transcription of both nuclear and mtDNA-encoded OXPHOS genes in the transition to the neonate.

Fourth, G elongation factor mitochondrial 1 (*GFM1*) was upregulated in the heart (six of seven organisms), although it was downregulated in the lizard heart and upregulated in the forebrain/cerebrum of two of six organisms, in the hindbrain/cerebellum of four of six organisms, in the kidney of six of seven organisms, and in the liver of three of eight organisms (Fig. 4). The upregulation of *GFM1* is of interest in the context of upregulated mitochondrial ribosomal proteins in the neonate. This raises the possibility that mitochondrial protein synthesis is also upregulated in the neonate.

The expression of *NRF1*, a known regulator of OXPHOS gene expression in the nucleus and of mitochondrial biogenesis (Gureev et al. 2019), was significantly downregulated in the liver of five of eight organisms (human, mouse, pig, rabbit, and rat) but was elevated in the chicken liver and downregulated in the kidney and forebrain/cerebrum of four of seven and four of six organisms, respectively (Fig. 4; Supplemental Fig. S38). This suggests that only a subset of the factors that regulate mitochondrial biogenesis form candidate regulatory factors to be involved in CMNGE after birth/hatching.

Finally, while considering the core mtDNA transcriptional regulatory factors, we noticed that *TFB2M* was significantly upregulated in the heart of six of seven organisms, in the forebrain/cerebrum of three of six organisms (chicken, rabbit, and rhesus), in the hindbrain/cerebellum of rhesus, in the kidney of three of seven organisms (mouse, rabbit, and rhesus), and in the liver of five of eight organisms (human, mouse, pig, rabbit, and rat) (Fig. 4; Supplemental Table S1). It is worth noting that *TFB2M* expression was significantly downregulated in chicken liver. Then, while considering mitochondrial transcription factor A (*TFAM*), we found that it was significantly downregulated after birth in the human heart ($\log_2$FC = −0.63); in forebrain/cerebrum samples from humans, rats, and rabbits ($\log_2$FC = −1.37, $\log_2$FC = −1.12, $\log_2$FC = −0.81, respectively); in the hindbrain/cerebellum of humans and rabbits ($\log_2$FC = −0.81, $\log_2$FC = −0.51, respectively); in the human and chicken kidney ($\log_2$FC = −0.5, $\log_2$FC = −0.34, respectively), and in the chicken liver ($\log_2$FC = −0.61, respectively) (Supplemental Fig. S38; Supplemental Table S1). Because in high cellular concentrations, TFAM coats the mtDNA and, in lower concentrations, it promotes mtDNA transcription and replication, it is conceivable that lower TFAM levels reduce mtDNA occupancy and increase mtDNA transcription and replication (Kukat et al. 2015). Consistent with this interpretation, the mitochondrial RNA polymerase (*POLRMT*) was significantly upregulated in the heart of humans, the mouse, and rat and in human kidney; these findings support the possibility that core mtDNA transcriptional machinery partially participates in the CMNGE upregulation after birth (Supplemental Table S1; Supplemental Fig. S38).

Taken together, the regulation of mitochondrial biogenesis seems the most prominent regulatory mechanism that responds similarly to the CMNGE shift in the neonate. Hence, it is conceivable that control of mitochondrial biogenesis is the main player that steers the mitochondrial–metabolic transition from fetus to neonate in mammals and in chicken.

Hypoxia and locomotion: assessment of altered pathways that likely require the upregulation of CMNGE after birth

Mammalian embryos develop in utero in hypoxic conditions (Webster and Abela 2007). Previous work revealed that animal exposure to hypoxia reduces mitochondrial metabolism and allows cardiomyocyte regeneration in the neonate and in the adult mouse heart (Nakada et al. 2017). Thus, we reasoned, that upregulation of CMNGE after birth mechanistically associates with the transition to an oxygen-rich environment and is important for the transition of embryonic to adult tissue. Therefore, as a first step, we tested for the expression of the top genes that are known to be upregulated in hypoxia in humans during development. Our results revealed a reduction in the expression of most of the genes that positively respond to hypoxia across tissues and species (Fig. 5; Supplemental Fig. S41). We also noticed that humans display a stronger reduction in the brain and liver compared with the heart and kidney.

Because the transition to the neonate is associated with an exit from a confined space (the womb, egg) to the external environment, we hypothesized that the expression of genes involved in the regulation of locomotion might be altered. While analyzing genes related to locomotion, we did not find a consistent overall change in expression (Supplemental Fig. S42). Because the forebrain harbors most neurons that direct locomotion (Ferreira-Pinto et al. 2018), our findings suggest that the upregulation of CMNGE in the forebrain may contribute to the emergence of locomotion. As the activity of proteins involved in locomotion is logically related to skeletal muscle, it would be of interest to study the expression of this pathway in muscle after birth when such data become available.

The lizard *A. carolinensis* did not show any consistent pattern in these pathways when comparing embryo to adult samples (Supplemental Figs. S33, S42–S44).

Together, the transition of the fetus from hypoxic conditions to breathing atmospheric oxygen might influence the OXPHOS gene expression after birth, whereas a shift in the mode of locomotion might not influence the OXPHOS gene expression in these tissues and organisms.

Elevation of mitonuclear gene expression before hatching associated with the initiation of spontaneous movement in *Xenopus tropicalis* and in *Drosophila melanogaster*

Although mammals and chicken displayed elevated CMNGE after birth, they did not show any clear CMNGE alteration before birth. We therefore asked whether putative changes in CMNGE during prenatal stages were masked by the major impact of postnatal samples. To address this possibility, we analyzed the same species, focusing only on prenatal samples before birth/hatching. This analysis did not reveal any consistent alteration in CMNGE among the tested species (mammals and chicken) during prenatal development (Supplemental Fig. S45). We next analyzed bulk RNA samples collected during embryonic and fetal development from two nonmammalian vertebrates—*Xenopus tropicalis* (tropical frog, with two experimental repeats) (Mitros et al. 2019) and *Danio rerio* (zebrafish) (Levin et al. 2016), as well as from two invertebrates—*Drosophila melanogaster* and *C. elegans* (whole organism) (Levin et al. 2016). *X. tropicalis* samples (whole organism) were collected from embryo cleavage stages until the tailbud free-swimming stage (Mitros et al. 2019), whereas *D. rerio*, *D. melanogaster*, and *C. elegans* were sampled from the cleavage stage until hatching (but not after). First, while analyzing mtDNA and nuclear DNA–encoded OXPHOS gene expression, we found that, unlike mammals and chicken, CMNGE elevation occurred in *X. tropicalis* before hatching (Fig. 6A; Supplemental Figs. S46–S48). In replicate one, both mtDNA and nuclear OXPHOS genes rose concurrently in

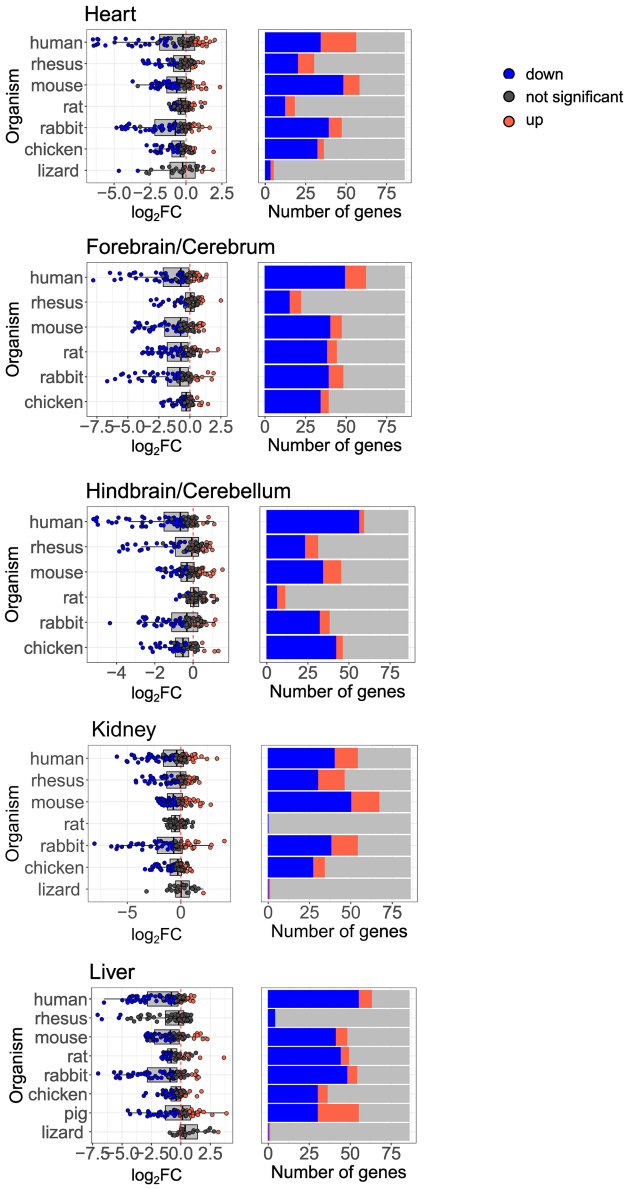

Figure 5. Hypoxia response gene expression is generally reduced after birth. (*Left*) Box plots representing the $\log_2$FC of hypoxia genes. The *x*-axis indicates $\log_2$FC values; *y*-axis, organisms. Color bar: blue dots indicate significant downregulation ($\log_2$FC < −0.2, *P*-value < 0.05); red dots, significant upregulation ($\log_2$FC > 0.2, *P*-value < 0.05); and black dots, nonsignificant. The dashed vertical red line corresponds to the value of zero $\log_2$FC on the *x*-axis. (*Right*) Bar plots representing the number of significant (upregulated in red, downregulated in blue) or insignificant genes (in gray). The *x*-axis indicates number of genes; *y*-axis, organisms tested.

timing and rate during developmental stages 24–26, whereas in replicate two, elevation occurred at stage 28 and aligned in timing, although with a distinct differential rate of elevated expression (Supplemental Figs. S47, S48). This early CMNGE coincided with initial motor neuron activity and spontaneous movement, respectively.

In *D. melanogaster*, elevated mtDNA genes expression was observed at 585 min postfertilization (mpf), whereas elevated expression of nuclear DNA–encoded structural OXPHOS genes was observed shortly later, 645 mpf (Fig. 6A; Supplemental Figs. S49, S50); the elevated expression of both genomes preceded the onset of muscle twitching (840 mpf; i.e., early movement) (Halpern et al. 1991; Crisp et al. 2008).

For *C. elegans*, mtDNA genes expression was elevated at 60 mpf (Supplemental Figs. S46, S51, S52); however, only a small subset of nuclear DNA–encoded OXPHOS structural genes showed transient upregulation at this point, which was not sustained throughout the remainder of prenatal development, suggesting limited coordination in early stages.

In *D. rerio* (zebrafish), mtDNA genes reached peak of expression at 3520 mpf in the window w = 4 (Fig. 6A; Supplemental Figs. S53, S54). Conversely, nuclear DNA–encoded OXPHOS genes peaked earlier at 280 mpf. Additionally, analyses across varied window sizes (from w = 4 to w = 20) indicated different time frames for mtDNA expression peaks, with the highest FCs shifting between 2120 and 3520 mpf. This variability suggests biphasic mtDNA expression elevation that may be independent of nuclear OXPHOS genes, implying more complex regulatory dynamics in this species during prenatal development.

As mentioned above, our analysis suggests that in *X. tropicalis* and in *D. melanogaster* the timing of elevated CMNGE is associated with the beginning of embryonic movement, thus tempting us to speculate a causal connection. However, our analysis of the expression of genes related to the locomotion pathway in these two species (Supplemental Fig. S55) revealed that only a small subset of the locomotion pathway genes displayed altered expression in the same time frame of CMNGE. Therefore, the association of CMNGE with the locomotive phenotype during development (e.g., beginning of embryonic movements) cannot be easily explained by overall analysis of the locomotion pathway. This underlines the need for a future study that will focus on the involvement of mitochondrial function in the regulation of muscle movement, while taking advantage of single cells analysis.

We next asked whether the elevation of CMNGE toward hatching is unique to OXPHOS or could be found in other mitochondrial pathways of metabolism. Our analysis revealed that the expression of TCA cycle enzymes and the mitochondrial ribosome genes were also elevated toward hatching in *X. tropicalis* and in *D. melanogaster* (Supplemental Figs. S56–S59). Glycolysis genes did not show any altered expression pattern toward hatching.

Next, we asked whether CMNGE that was observed toward hatching in *D. melanogaster* and *X. tropicalis* is modulated by mitochondrial transcription factors, RNA binding factors, or biogenesis regulatory factors (Fig. 6B; Supplemental Fig. S46). The results highlighted three candidate regulatory genes that were shared between *D. melanogaster* and *X. tropicalis* (in two independent data sets): mitochondrial translation elongation factor (*TUFM*), *PTCD3* (binds mtDNA-encoded rRNAs and regulator of mitochondrial translation), and *LRPPRC* (regulator of mitochondrial RNA stability). *YY1*, a known regulator of OXPHOS nuclear gene expression (Nandi et al. 2020), showed reduced expression in *D. melanogaster* and *X. tropicalis*, thus excluding it from positive involvement in regulating the elevated CMNGE during development in these species. An additional gene that displayed reduced expression in these organisms is *SIN3A*, a transcriptional repressor protein known to regulate mitochondrial components. Consistent with this finding, a previous study showed that loss of *SIN3* in *D. melanogaster* cultured cells resulted in upregulation of both nuclear DNA–encoded and mtDNA-encoded genes (Barnes et al. 2010). Hence, *D. melanogaster* and *X. tropicalis* likely share a mechanism controlling CMNGE during prenatal development.

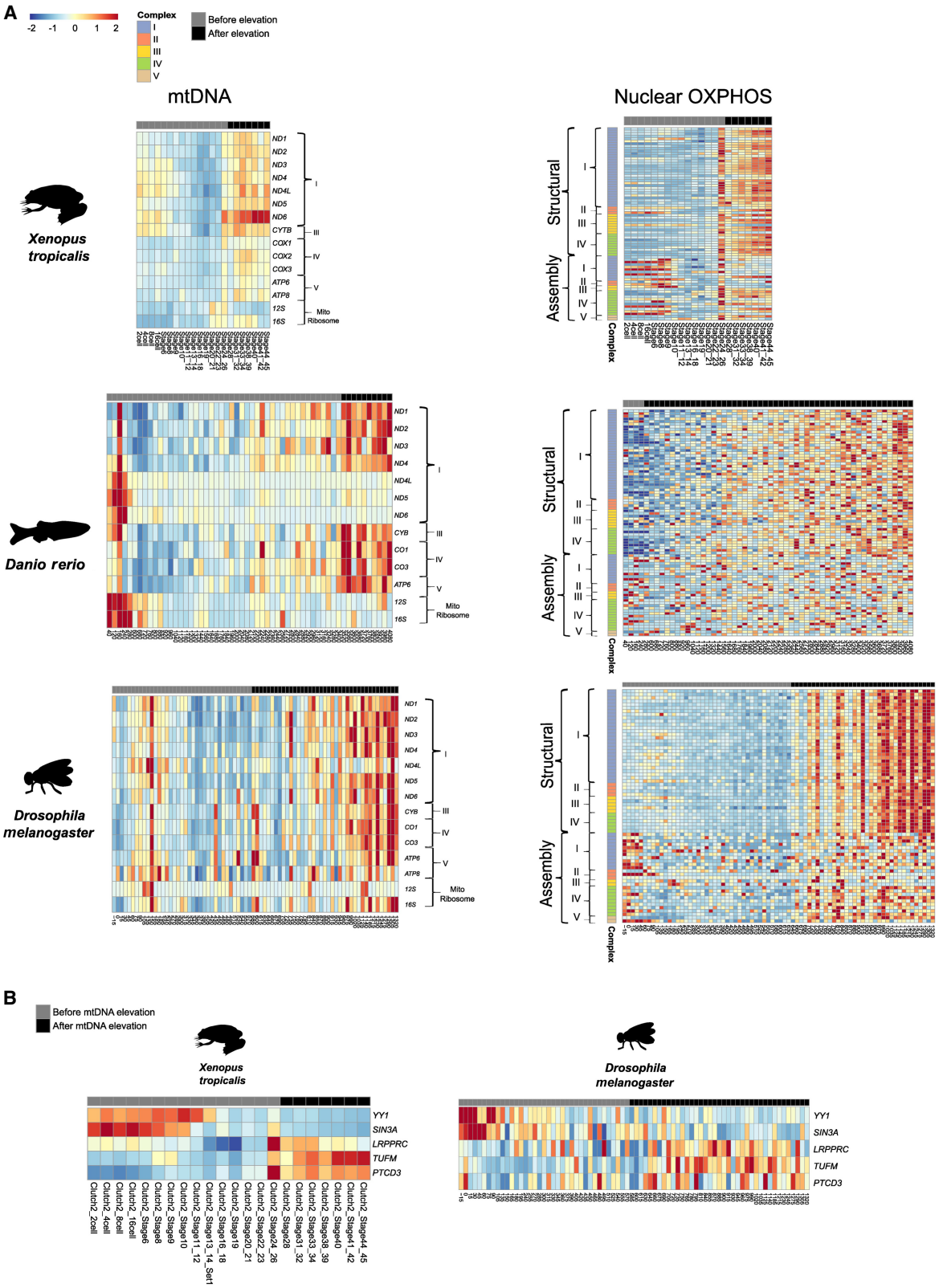

Figure 6. Mitonuclear gene expression is elevated during prenatal development. (*A*) Heatmaps of mtDNA and nuclear DNA–encoded OXPHOS gene expression from *X. tropicalis*, *C. elegans*, *D. melanogaster*, and *D. rerio*. The color bar indicates the scaled expression. Red scale indicates elevated expression; blue scale, reduced expression. The *x*-axis indicates prenatal samples; *y*-axis, mtDNA/OXPHOS genes. Notice division into OXPHOS complexes and into structural and assembly genes of the OXPHOS. (*B*) Heatmap representing $\log_2$FC values of regulatory factors and genes related to mitochondrial biogenesis. The color bar indicates the $\log_2$FC. The *x*-axis indicates organisms; *y*-axis, genes. Only $\log_2\text{FC} > 0.2$ and $\log_2\text{FC} < -0.02$ are shown.

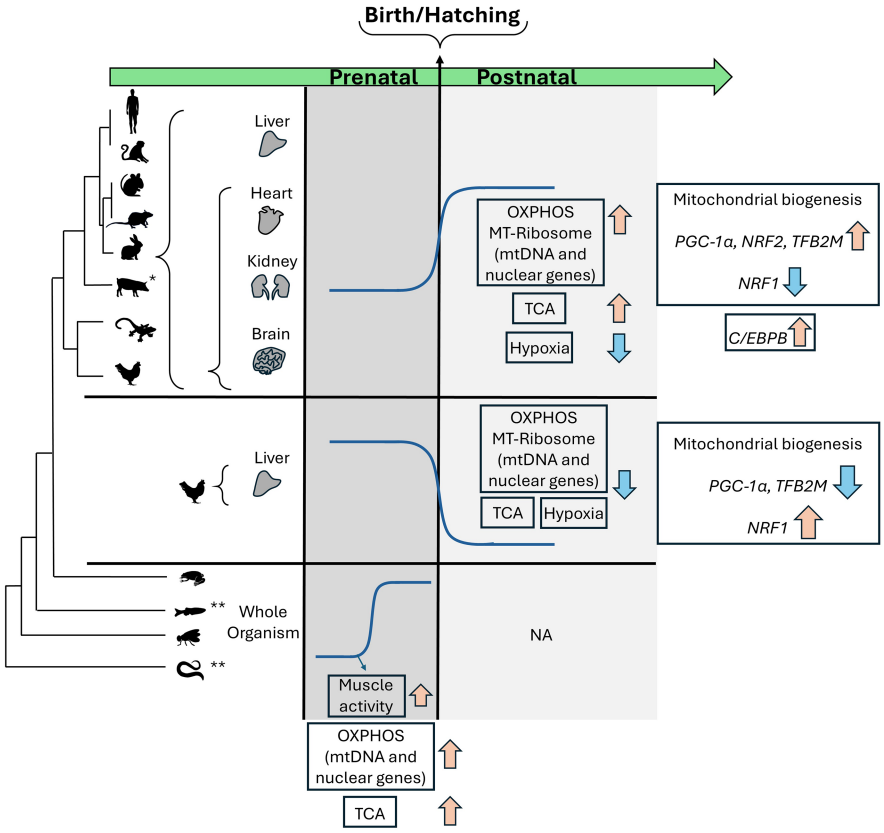

Figure 7. The landscape of CMNGE during development across metazoan evolution. OXPHOS, mitochondrial ribosome, and TCA genes show elevated expression right after birth in mammals chicken (after hatching, apart from the liver), and in the lizard across tissues. This pattern is associated with elevated expression of regulators of mitochondrial biogenesis and with transition from hypoxia to normoxia. The frog and *Drosophila* show elevated CMNGE in association with the start of locomotion in the embryos. Blue arrows indicate downregulation; orange arrows, upregulation; and gray areas, elevated or reduced mitonuclear gene expression. (*) *S. scroffa* (pig) samples were available only from the liver. (**) *D. rerio* (zebrafish) and *C. elegans* did not show clear CMNGE.

Discussion

In the current study, we assessed the cross talk between prenatal development and regulation of mitochondrial function at the RNA level during metazoan evolution across multiple tissues (Fig. 7). Our analysis showed a concomitant increase of both mtDNA and nuclear DNA–encoded OXPHOS gene expression either immediately or shortly after birth (mammals) or after hatching (*G. gallus* and *A. carolinensis*). It was previously shown that the transition from the fetus to the neonate in the mouse heart requires a postnatal metabolic switch to OXPHOS (Talman et al. 2018; Zhao et al. 2019; Secco and Giacca 2023), as well as profound alterations of mitochondrial protein functions in the early postnatal period (Talman et al. 2018). Our findings argue for a general, cross-tissue, and evolutionarily conserved elevation in mitochondrial function after birth; our results imply that the transition of the embryo to the neonate most probably relies on CMNGE. While considering OXPHOS, most of the elevated CMNGE was observed in structural OXPHOS subunits rather than in the assembly genes. This suggests that CMNGE involves the former, implying that OXPHOS assembly genes are regulated differently from the structural OXPHOS genes during development. Second, along with the elevated mitonuclear gene expression after birth, we observed elevated expression of major mitochondrial metabolic pathways, such as the mitochondrial ribosome and TCA cycle enzymes. Moreover, the mtDNA copy number was reported to have significantly increased in postnatal human liver and muscle, supporting a general increase in mitochondrial mass after birth (Pejznochova et al. 2010). As we did not observe consistent change in the expression of mtDNA replication factors after birth (Supplemental Table S1), the reported change in mtDNA copy number might only reflect change in mitochondrial mass rather than mtDNA replication. Finally, we noticed that the CMNGE alteration after birth/hatching was evident in somatic tissues but less in the reproductive organs (testis and ovary), apart from certain organisms (Supplemental Fig. S7). Because reproductive organs become more active upon puberty, it would be of interest to assess mitochondrial gene expression in reproductive organs before and after puberty. Additionally, because mitonuclear gene expression is likely coordinated also at the level of single cells (Medini et al. 2021a), it would be of interest to assess the mitonuclear gene expression in different cell types and to perform scRNA-seq analysis before and after birth from different tissues, hopefully from a variety of organisms. Finally, it would also be of interest to assess in future experiments whether elevated CMNGE after birth is also reflected at the protein level, especially in light of the claim for a strong impact of mitochondrial translation on the coregulation of the two genomes (McShane et al. 2024). Taken together, our results strongly support a regulatory basis underlying the coordinated response of mitochondrial and nuclear OXPHOS gene expression at the RNA level to the transition from fetal to neonatal life. Furthermore, although the association between the elevated gene expression in both genomes during development is correlative, its conservation across species and prevalence in different tissues strongly suggests a mechanistic basis for coordination.

One clear exception from the coordinated upregulation is the chicken liver: Unlike the elevated CMNGE in mammalian liver samples, the chicken liver showed reduced CMNGE. After hatching, the chick's main source of energy is derived from the conversion of feed-based carbohydrates into fatty acids, which mainly occur in the liver, as in humans (Noble and Cocchi 1990; Hicks et al. 2022). However, unlike humans and other mammals that harbor adipocytes in a variety of body sites, much of the fat of the chick is stored in the liver (Leveille 1969). It is thus conceivable that the hepatic molecular metabolic response to posthatching in the chicken involves an increase in lipolysis-related gene expression (Latour et al. 1995). This is different from the mammalian neonatal liver, which performs uptake of fatty acids from maternal milk, esterification of fatty acids into triglycerides, and storage in

lipid droplets. These differences may impact the usage and underlying regulatory difference of CMNGE in the chick versus neonatal liver upon birth/hatching. Regardless, mitonuclear gene expression is coordinately increased (mammals) or reduced (chicken), again supporting an underlying regulatory mechanism.

Although OXPHOS genes are upregulated in the *A. carolinensis* heart, this pattern was not consistently observed in other mitochondrial pathways. This suggests a species-specific regulation of mitochondrial gene expression in lizards, which calls for further exploration of metabolic gene expression across the development of other additional lizard species. Once gene expression data sets become publicly available from several lizard species, such study may shed light on the dynamic of mitochondrial gene expression and on the underlying regulation of metabolism, across vertebrates.

To identify the best candidate factors to regulate the altered CMNGE after birth/hatching, we screened a compendium of known regulators of transcription, post-transcription, and mitochondrial biogenesis that displayed expression changes after birth across tissues and across evolution. Our findings highlighted an elevation of *PPARGC1A* expression, a major regulator of mitochondrial biogenesis (see more below), right after birth in many tissues and most organisms (apart from the human heart). In contrast, the chicken liver displayed a decrease in *PPARGC1A* expression, the very same pattern observed for mitonuclear gene expression. With this in mind, we also found that the expression pattern of *NRF2*, a known transcriptional regulator of nuclear DNA–encoded OXPHOS genes, which regulates *PPARGC1A* transcription and numerous respiratory chain genes, including cytochrome c oxidase (*COX*) components (Scarpulla 2002; Gureev et al. 2019), also followed the mitonuclear gene expression pattern across tissues and tested organisms. Whereas *NRF2* expression was elevated in the heart of most tested organisms, *PPARGC1A* expression was not, suggesting that the upregulation of *NRF2* in the heart after birth might be regulated by other factors. This interpretation should be tested in the future.

PPARGC1A acts as a transcriptional activator via protein–protein interactions with DNA-bound transcription factors (Tavares et al. 2020). Previous study showed that impaired *PPARGC1A* in mouse hearts led to reduced growth, arrested mitochondrial development late in gestation, and high lethality shortly after birth (Lai et al. 2008). As current data support the limitation of *PPARGC1A* activity to the nucleus, it is plausible that its involvement in regulation of mitonuclear gene expression occurs via regulating the regulators of both mitochondrial and nuclear OXPHOS genes. This thought is partially supported by our observed elevated expression of the mitochondrial RNA polymerase, *POLRMT*, in certain tissues and species; *POLRMT* is indirectly regulated by *PPARGC1A* (Wu et al. 1999; Gureev et al. 2019). The expression of *TFB2M*, a mtDNA transcription initiation factor that interacts with *POLRMT* (Falkenberg et al. 2002), was elevated after birth/hatching, and its transcription is regulated by *NRF2* (Gleyzer et al. 2005). In addition to *PPARGC1A*, *PPARGC1B* (*PGC-1beta*), a known transcriptional regulator of mitochondrial functions (Shao et al. 2010), was significantly upregulated across organs and species. These pieces of evidence suggest that the modulators of mitochondrial biogenesis form strong candidates to regulate CMNGE during the transition to postnatal life.

Nevertheless, this interpretation is limited by the following: Although *PPARGC1A* is known to increase the expression of both *NRF1* and *NRF2* mRNAs (Wu et al. 1999; Gureev et al. 2019; Popov 2020), we found that the expression of *NRF1* was decreased after birth across tissues and organisms. Therefore, only some regulators of mitochondrial biogenesis are candidates to associate with the regulation of CMNGE after birth.

The expression of *CEBPB* was consistently upregulated after birth in most tissues and organisms tested, apart from the chicken liver. Unlike *PPARGC1A* and *PPARGC1B*, *CEBPB* has been in vivo localized both to the nucleus and to the mitochondria in cells, thus serving as an attractive candidate to directly participate in CMNGE. This interpretation awaits support from future silencing and overexpression experiments of *CEBPB* in cells, which will enable direct assessment of the impact of *CEBPB* on CMNGE.

Because CMNGE after birth and hatching is common to all mammals, the chicken, and the lizard, we reasoned that there should be a common condition in the transition to the neonate, or neonatal phenotype, that probably requires such a sharp and conserved shift in mitochondrial function. The first condition to be considered is the transition from hypoxia to breathing atmospheric oxygen. With this in mind, it is important to mention that hypoxia suppressed the activity of *PPARGC1A* and reduced its mRNA levels in cell lines (LaGory et al. 2015). Furthermore, hypoxia-inducible factor (*HIF*) is essential for mediating *PPARGC1A* suppression in hypoxia (LaGory et al. 2015), which is consistent with upregulation of *PPARGC1A* upon birth. However, this explanation is likely tissue specific in some organisms, as we found a tissue-dependent response of hypoxia regulatory factors after birth: Although, as expected, most of the hypoxia genes were downregulated in the human brain, liver, and kidney, the human heart displayed a weaker effect in the expression of hypoxia-responsive genes after birth. As the heart experiences a sudden elevation in oxygen levels after birth, one would expect a hypoxic response in the heart after birth owing to oxidative stress (Secco and Giacca 2023) and in response to hypoxia, an elevated mitochondrial energy production in cardiac cells (Essop 2007). Therefore, despite the weaker reduction in the hypoxia pathway in the human heart, our findings suggest that hypoxia may explain the need for elevated CMNGE after birth. With this in mind, it is conceivable that species-specific regulatory mechanisms are also important for regulating mitochondrial function during development, especially while considering the differences in the physiological requirements of different organisms. As more gene expression data sets become available for additional species, future analyses will allow us to better delineate these unique patterns and their potential biological significance.

Although we did not identify a clearly consistent change in CMNGE during prenatal development of mammals and chicken, we asked whether such changes could be identified in more distant metazoans, including vertebrates and invertebrates. In *X. tropicalis*, synchronized mtDNA and nuclear OXPHOS gene elevated expression aligns with the onset of motor activity. Similarly, in *D. melanogaster*, the coregulation between these gene sets precedes muscle twitches (Crisp et al. 2008), suggesting an associated need for muscle movement with the regulation of energy production in both the fly and the frog. Nevertheless, this interpretation is limited by the ambiguous mitonuclear gene expression coordination in *D. rerio* and in *C. elegans*. Thus, the connection between CMNGE and the emergence of movement during development emphasizes the need to study mitonuclear gene expression in a larger set of metazoans. Association between the upregulation of CMNGE and the initiation of locomotion is especially attractive because many mitochondrial disorders display impaired movement phenotypes (Tranchant and Anheim 2016; Ticci et al. 2021), further emphasizing the importance of the study of

CMNGE in such disorders, an interpretation that should be tested in future experiments.

In summary, our study revealed coordination of gene expression between the mitochondria and the nucleus in the transition from fetal to neonatal life and, for the first time, identified its conservation in vertebrates. Such conservation implies similar selective constraints across evolution and, hence, functional importance. Unexpectedly, our analysis revealed elevated CMNGE, which reflected a conserved metabolic shift postbirth (mammals) or hatching (bird and lizard). Key regulatory factors, for example, *PPARGC1A*, *PPARGC1B*, *NRF2*, *TFB2M*, and *CEBPB*, emerge as potential regulators of such CMNGE shifts. The identification of these factors as candidates to regulate CMNGE across species forms a testable hypothesis, which can be experimentally addressed while manipulating the expression of these factors in cells and organisms. Second, we found that elevated CMNGE preceded the initiation of locomotion in the frog and *Drosophila*. Our findings pave the path toward future identification of the underlying mechanism of CMNGE during development, as well as in particular tissues, during the course of evolution.

Methods

Data availability

Data source details and number of samples per analyzed data set are indicated in Table 1.

For Data set I, bulk RNA-seq FASTQ files were downloaded from ArrayExpress (https://www.ebi.ac.uk/arrayexpress/) with the following accession codes: E-MTAB-6769 (*G. gallus*), E-MTAB-6782 (*O. cuniculus*) E-MTAB-6798 (*M. musculus*), E-MTAB-6811 (*R. norvegicus*), E-MTAB-6813 (*M. mulatta*), and E-MTAB-6814 (*H. sapiens*) (Cardoso-Moreira et al. 2019). For data analysis, see the RNA-seq Analyses section. Data set I included 1346 RNA-seq libraries, encompassing embryo, fetal, and neonatal development in seven organs, nine to 23 developmental stages, depending on the analyzed organism. Samples that were collected during the same developmental week were considered biological replicates. For instance, samples that were generated from Carnegie stages 13 and 14 in a given organism were considered as replicates (4 weeks postconception [wpc]), as previously reported (Cardoso-Moreira et al. 2019). Accordingly, the data included one to four replicates per stage. Briefly, human prenatal samples were available at 4 wpc and for each week until 20 wpc (except for 14, 15, and 17 wpc). It is worth noting that there were no human samples available between 20 and 38 wpc. Postnatal human samples included "infants" (6–9 months old), "toddlers" (2–4 years old), "school" (7–9 years old), "teenagers" (13–19 years old), and adults from each decade until 63 years of age. Human ovary samples were collected only from prenatal samples (until 18 wpc), and therefore did not present insight into the transition to the neonate. Finally, the human kidney was sampled during development up until 8 years of age (hereby termed "school"). Samples from rhesus monkey (*M. mulatta*) were collected while taking into account that gestation lasts ~167 days. These samples were collected starting from fetal stage e93 in addition to four subsequent stages prior to birth (until e130). Notice that samples for the rhesus monkey were not available for e130 and e160. When considering the mouse (*M. musculus*), samples were collected from e10.5 and during subsequent days, each day, until birth (i.e., until e18.5). Postnatal mouse samples included P0, P3, P14, P28, and P63. For the rabbit, *O. cuniculus* (outbred New Zealand breed) samples were collected starting from e12 and the subsequent 11 time points up until (including) e27, while taking into account that gestation length is 29–32 days. Postnatal rabbit samples included P0, P14, and P84 and between P186 and P548. For the rat, *R. norvegicus* (outbred strain Holtzman SD) samples were collected starting from e11 and at subsequent daily time points until birth (until e20). Postnatal samples include P0, P3, P7, P14, P42, and P112. For the chicken, *G. gallus* (red junglefowl) egg incubation lasts ~21 days. Thus, collection time series started at e10 and at subsequent three additional stages until e17. Postnatal samples include P0, P7, P35, P70, and P155.

Data set II included RNA-seq experimental data collected during *S. scroffa* (pig) liver development. The data comprised a normalized count matrix of processed transcripts per million (TPM), which was downloaded from the Gene Expression Omnibus (GEO; https://www.ncbi.nlm.nih.gov/geo/) accession number GSE176387. We analyzed five developmental stages from porcine liver: E38, E80, the day of birth (0d), weaning at 28 days, sexual maturity at 110 days, with six replicates in each stage.

For Data set III, the fragments per kilobase million normalized count matrix was downloaded from GEO accession number GSE121019. We analyzed three developmental stages available for chicken liver: e13 and postnatal stages at 5 weeks and 42 weeks of age, with each having three replicates.

For Data set IV, the raw read count matrix was downloaded from GEO accession number GSE58455. We analyzed seven independently collected e13.5 samples and 12 adult samples (six at 6 weeks of age, six at 16 weeks of age) from mouse heart.

For Data set V (*A. carolinensis*), we took into account that *A. carolinensis* development typically lasts 30–33 days and includes 19 stages (Sanger et al. 2008). Raw bulk RNA-seq FASTQ files were downloaded from GEO accession number GSE97367. We analyzed 22 embryonic samples (from stages 15–16) and 30 adult samples from four organs (brain, heart, kidney, liver) and 26 whole embryonic samples.

For Data set VI (*X. tropicalis*), raw data FASTQ files were downloaded from GEO accession number GSE37452. The samples included two clutches: (1) from two cells to stage 45, and (2) from stage 9 to stage 42. These stages span from the beginning of cleavage to the tailbud free swimming stage. In all cases, the whole organism was sampled.

For Data set VII, raw read count matrices for the zebrafish (*D. rerio*), *D. melanogaster*, and *C. elegans* were downloaded from GEO accession number GSE70185 (Levin et al. 2016). Time series included samples from the cleavage stage up to the time point prior to hatching.

RNA-seq analyses: mapping, read count and control for nuclear mitochondrial sequences

For Data sets I, V, and VI, FASTQ files were mapped, and read counts were generated for further analyses (see below). For Data sets II, III, IV, and VII, we downloaded normalized postmapping read count files for subsequent analyses.

Specifically, for further analyses of Data sets I, V, and VI, sequenced reads were trimmed using Trim Galore! (version 0.4.5; https://www.bioinformatics.babraham.ac.uk/projects/trim_galore/). Prior to read count analyses, we controlled for possible noise originating from nuclear mitochondrial fragments (NUMTs), for example, mtDNA sequence fragments that were transferred from the mitochondria to the nucleus during the course of time (Mishmar et al. 2004). NUMTs potentially pose an obstacle to mtDNA gene expression assessment, as a subset of RNA reads, particularly those that are relatively recent (Mishmar et al. 2004), might be more similar to the active mtDNA and sequencing reads from mtDNA genes; such fragments might be erroneously filtered out while applying the unique mapping protocol. To overcome such a problem, reads were first mapped solely against the

mtDNA genome using BWA using the aln parameter (BWA-backtrack algorithm) (Li and Durbin 2009); then, the reads that did not map to the mtDNA were uniquely mapped against the entire reference genome of the relevant organisms using STAR (version 2.5.3), while employing default parameters and the parameter [—outFilterMultimapNmax 1] (Dobin et al. 2013). Expression levels of all genes were counted using HTSeq-count v0.11.2 (Anders et al. 2015) using default parameters while employing the [-f bam] parameters. High-quality samples were used as listed in the original study (Cardoso-Moreira et al. 2019).

Libraries with nonzero read counts of mtDNA genes were used for subsequent analysis to avoid technical noise. Reference genomes that were used are listed in Supplemental Table S2.

Quantification of gene expression and statistical analysis

Read count data matrices were normalized using DESeq2 normalization method available from the DESeq2 R package (R Core Team 2013; Love et al. 2014). For Data set I, we used a median of two to four replicates for each stage for statistics. Heatmaps were created using the pheatmap R package (https://github.com/raivokolde/pheatmap; R Core Team 2013). To assess mtDNA gene expression across developmental stages, a sliding window algorithm was employed with varying window sizes: w = 2, w = 4, and w = 6. FC values for each mtDNA gene were computed over specific time point intervals. For w = 2, the FC was calculated between consecutive time points (e.g., from time point 1 to time point 2, followed by time point 2 to time point 3, etc.). For w = 4, the FC was determined by the median of the first two time points and the median of the subsequent two time points to capture broader temporal shifts. Similarly, for w = 6, the FC was calculated between the median of three subsequent time points to the following ones, providing a wider context for temporal changes. The smaller window size allows for more sensitive detection of rapid changes in expression (with higher signal-to-noise), whereas the larger window size emphasizes longer-term trends.

During data analysis, the average FC for mtDNA genes was computed for each time point to identify those exhibiting the highest mean FC values, thereby highlighting significant expression changes.

Window sizes w = 4 and w = 6 showed similar trends; however, given the limited number of time points in *G. gallus* (usually n = 9), using w = 6 would reduce resolution and potentially obscure key shifts in gene expression. Window w = 2, on the other hand, introduced more noise. Therefore, for the sake of consistency, w = 4 was chosen for the analysis across species, offering sufficient resolution in all tested organisms.

In nonmammalian species, including *X. tropicalis*, *D. melanogaster, D. rerio*, and *C. elegans*, the sliding window range was extended to incorporate sizes from w = 2 to w = 20, utilizing only even-numbered windows to ensure an equal number of samples in each iteration. This strategy accommodated variations in the number of sampled developmental stages across these species compared to mammals and birds.

The overall "topography" of mtDNA gene expression graphs remained consistent across the different window sizes used, suggesting that the chosen window size did not significantly impact the analysis outcomes. Again, window w = 4 was chosen to ensure a consistent analysis across species. To assess whether the change in FC was coordinated with nuclear DNA–encoded OXPHOS gene expression, we conducted the same analysis to this set of genes.

Supplemental Figures S1–S6, S13–S18, S21–S26, and S47–S54 present the results of the analysis across all window sizes, enabling a detailed and accurate representation of mtDNA, nuclear OXPHOS, and structural OXPHOS gene expression patterns over time, respectively, while maintaining consistency in the analysis across species.

Differential expression of mitochondrial genes in a given time point was calculated (DESeq2) separately for each data set, while considering samples from the previous and subsequent time points. Correction for multiple testing for each specified set of genes was performed using an adjusted *P*-value of 0.05. Box plot and bar plot graphs were generated using "ggplot2" (Wickham 2016) and RColorBrewer R packages (R Core Team 2013). Tables were generated using the R packages openxlsx, tidyr, and reshape2 (R Core Team 2013; Zhang 2016). The level of coordination of mitonuclear genes was calculated as follows: the number of significantly upregulated OXPHOS genes (X_{up}) minus the number of significantly downregulated OXPHOS genes (X_{down}), divided by the number of total available OXPHOS genes, as in the following formula:

$$\frac{X_{up} - X_{down}}{X_{total}}.$$

Expression of genes was considered significantly altered if their adjusted *P*-value was smaller than 0.05 and the absolute value of $\log_2$FC was greater than 0.2.

GO terms used in the analysis

The following Gene Ontology (GO) Terms were used to download and perform differential expression analysis: genes belonging to "TCA" (GO:0006099), "glycolytic process" (GO:0006096), ROS formation (GO:1903409), "locomotion" (GO:0040011), and "positive regulation of cellular response to hypoxia" (GO:1900039). We assessed the expression of candidate mtDNA regulatory factors of transcription, regulatory factors of mtDNA replication, and nuclear DNA–encoded factors with known mitochondrial RNA-binding activity (Wolf and Mootha 2014; Cohen et al. 2016), in addition to RNA- and DNA-binding proteins that were recently identified in human mitochondria (Ardail et al. 1993; Fernández-Vizarra et al. 2008; She et al. 2011; Blumberg et al. 2014; Lambertini et al. 2015; Chatterjee et al. 2016). The hypoxia gene set was downloaded from a previous study (Bono and Hirota 2020). Accordingly, the top 100 responding genes to hypoxia with the highest score in humans were used for the analyses.

Competing interest statement

The authors declare no competing interests.

Acknowledgments

This work was funded by grants from the Israeli Science Foundation (ISF 404/21) and from the life sciences division of the US Army Research Office (grant no. 80581-BB) awarded to D.M. We thank the Myles Thaler Genetics and Genomics Research cathedra, BGU, for supporting this research. We thank Ben-Gurion University for awarding H.M. the Negev scholarship for excellent PhD students and a short-term postdoc training grant.

Author contributions: H.M. performed all analyses and participated in all stages of writing the paper. D.M. conceived the idea of the study, supervised the analyses, and wrote the paper.

References

Anders S, Pyl PT, Huber W. 2015. HTSeq: a Python framework to work with high-throughput sequencing data. *Bioinformatics* **31:** 166–169. doi:10.1093/bioinformatics/btu638

Ardail D, Lerme F, Puymirat J, Morel G. 1993. Evidence for the presence of alpha and beta-related T3 receptors in rat liver mitochondria. *Eur J Cell Biol* **62:** 105–113.

Barnes VL, Strunk BS, Lee I, Hüttemann M, Pile LA. 2010. Loss of the SIN3 transcriptional **c**orepressor results in aberrant mitochondrial function. *BMC Biochem* **11:** 26. doi:10.1186/1471-2091-11-26

Barreto FS, Watson ET, Lima TG, Willett CS, Edmands S, Li W, Burton RS. 2018. Genomic signatures of mitonuclear coevolution across populations of *Tigriopus californicus*. *Nat Ecol Evol* **2:** 1250–1257. doi:10.1038/s41559-018-0588-1

Barshad G, Blumberg A, Cohen T, Mishmar D. 2018. Human primitive brain displays negative mitochondrial-nuclear expression correlation of respiratory genes. *Genome Res* **28:** 952–967. doi:10.1101/gr.226324.117

Bar-Yaacov D, Hadjivasiliou Z, Levin L, Barshad G, Zarivach R, Bouskila A, Mishmar D. 2015. Mitochondrial involvement in vertebrate speciation? The case of mito-nuclear genetic divergence in chameleons. *Genome Biol Evol* **7:** 3322–3336. doi:10.1093/gbe/evv226

Blumberg A, Sri Sailaja B, Kundaje A, Levin L, Dadon S, Shmorak S, Shaulian E, Meshorer E, Mishmar D. 2014. Transcription factors bind negatively selected sites within human mtDNA genes. *Genome Biol Evol* **6:** 2634–2646. doi:10.1093/gbe/evu210

Bono H, Hirota K. 2020. Meta-analysis of hypoxic transcriptomes from public databases. *Biomedicines* **8:** 10. doi:10.3390/biomedicines8010010

Burch HB, Lowry OH, Kuhlman AM, Skerjance J, Diamant EJ, Lowry SR, Von Dippe P. 1963. Changes in patterns of enzymes of carbohydrate metabolism in the developing rat liver. *J Biol Chem* **238:** 2267–2273. doi:10.1016/S0021-9258(19)67964-0

Cardoso-Moreira M, Halbert J, Valloton D, Velten B, Chen C, Shao Y, Liechti A, Ascenção K, Rummel C, Ovchinnikova S, et al. 2019. Gene expression across mammalian organ development. *Nature* **571:** 505–509. doi:10.1038/s41586-019-1338-5

Chan JY, Kwong M, Lu R, Chang J, Wang B, Yen TS, Kan YW. 1998. Targeted disruption of the ubiquitous CNC-bZIP transcription factor, Nrf-1, results in anemia and embryonic lethality in mice. *EMBO J* **17:** 1779–1787. doi:10.1093/emboj/17.6.1779

Charmpilas N, Tavernarakis N. 2020. Mitochondrial maturation drives germline stem cell differentiation in *Caenorhabditis elegans*. *Cell Death Differ* **27:** 601–617. doi:10.1038/s41418-019-0375-9

Chatterjee A, Seyfferth J, Lucci J, Gilsbach R, Preissl S, Böttinger L, Mårtensson CU, Panhale A, Stehle T, Kretz O. 2016. MOF acetyl transferase regulates transcription and respiration in mitochondria. *Cell* **167:** 722–738.e23. doi:10.1016/j.cell.2016.09.052

Chen L, Li J, Yuan R, Wang Y, Zhang J, Lin Y, Wang L, Zhu X, Zhu W, Bai J, et al. 2022. Dynamic 3D genome reorganization during development and metabolic stress of the porcine liver. *Cell Discov* **8:** 56. doi:10.1038/s41421-022-00416-z

Cohen T, Levin L, Mishmar D. 2016. Ancient out-of-Africa mitochondrial DNA variants associate with distinct mitochondrial gene expression patterns. *PLoS Genet* **12:** e1006407. doi:10.1371/journal.pgen.1006407

Crisp S, Evers JF, Fiala A, Bate M. 2008. The development of motor coordination in *Drosophila* embryos. *Development* **135:** 3707–3717. doi:10.1242/dev.026773

Deng X, Lin N, Fu J, Xu L, Luo H, Jin Y, Liu Y, Sun L, Su J. 2020. The Nrf2/PGC1alpha pathway regulates antioxidant and proteasomal activity to alter cisplatin sensitivity in ovarian cancer. *Oxid Med Cell Longev* **2020:** 4830418. doi:10.1155/2020/4830418

Dobin A, Davis CA, Schlesinger F, Drenkow J, Zaleski C, Jha S, Batut P, Chaisson M, Gingeras TR. 2013. STAR: ultrafast universal RNA-seq aligner. *Bioinformatics* **29:** 15–21. doi:10.1093/bioinformatics/bts635

Essop MF. 2007. Cardiac metabolic adaptations in response to chronic hypoxia. *J Physiol* **584:** 715–726. doi:10.1113/jphysiol.2007.143511

Falkenberg M, Gaspari M, Rantanen A, Trifunovic A, Larsson NG, Gustafsson CM. 2002. Mitochondrial transcription factors B1 and B2 activate transcription of human mtDNA. *Nat Genet* **31:** 289–294. doi:10.1038/ng909

Fernández-Vizarra E, Enriquez JA, Pérez-Martos A, Montoya J, Fernández-Silva P. 2008. Mitochondrial gene expression is regulated at multiple levels and differentially in the heart and liver by thyroid hormones. *Curr Genet* **54:** 13–22. doi:10.1007/s00294-008-0194-x

Ferreira-Pinto MJ, Ruder L, Capelli P, Arber S. 2018. Connecting circuits for supraspinal control of locomotion. *Neuron* **100:** 361–374. doi:10.1016/j.neuron.2018.09.015

Folmes CD, Nelson TJ, Martinez-Fernandez A, Arrell DK, Lindor JZ, Dzeja PP, Ikeda Y, Perez-Terzic C, Terzic A. 2011. Somatic oxidative bioenergetics transitions into pluripotency-dependent glycolysis to facilitate nuclear reprogramming. *Cell Metab* **14:** 264–271. doi:10.1016/j.cmet.2011.06.011

Gershoni M, Templeton AR, Mishmar D. 2009. Mitochondrial bioenergetics as a major motive force of speciation. *Bioessays* **31:** 642–650. doi:10.1002/bies.200800139

Gleyzer N, Vercauteren K, Scarpulla RC. 2005. Control of mitochondrial transcription specificity factors (TFB1M and TFB2M) by nuclear respiratory factors (NRF-1 and NRF-2) and PGC-1 family coactivators. *Mol Cell Biol* **25:** 1354–1366. doi:10.1128/MCB.25.4.1354-1366.2005

Gureev AP, Shaforostova EA, Popov VN. 2019. Regulation of mitochondrial biogenesis as a way for active longevity: interaction between the Nrf2 and PGC-1alpha signaling pathways. *Front Genet* **10:** 435. doi:10.3389/fgene.2019.00435

Halpern M, Chiba A, Johansen J, Keshishian H. 1991. Growth cone behavior underlying the development of stereotypic synaptic connections in *Drosophila* embryos. *J Neurosci* **11:** 3227–3238. doi:10.1523/JNEUROSCI.11-10-03227.1991

Hance N, Ekstrand MI, Trifunovic A. 2005. Mitochondrial DNA polymerase gamma is essential for mammalian embryogenesis. *Hum Mol Genet* **14:** 1775–1783. doi:10.1093/hmg/ddi184

Hanson RW, Reshef L. 1997. Regulation of phosphoenolpyruvate carboxykinase (GTP) gene expression. *Annu Rev Biochem* **66:** 581–611. doi:10.1146/annurev.biochem.66.1.581

Hicks JA, Pike BE, Liu HC. 2022. Alterations in hepatic mitotic and cell cycle transcriptional networks during the metabolic switch in broiler chicks. *Front Physiol* **13:** 1020870. doi:10.3389/fphys.2022.1020870

Hill GE, Havird JC, Sloan DB, Burton RS, Greening C, Dowling DK. 2019. Assessing the fitness consequences of mitonuclear interactions in natural populations. *Biol Rev* **94:** 1089–1104. doi:10.1111/brv.12493

Hom JR, Quintanilla RA, Hoffman DL, de Mesy Bentley KL, Molkentin JD, Sheu SS, Porter GA Jr. 2011. The permeability transition pore controls cardiac mitochondrial maturation and myocyte differentiation. *Dev Cell* **21:** 469–478. doi:10.1016/j.devcel.2011.08.008

Kim TH, Hur EG, Kang SJ, Kim JA, Thapa D, Lee YM, Ku SK, Jung Y, Kwak MK. 2011. NRF2 blockade suppresses colon tumor angiogenesis by inhibiting hypoxia-induced activation of HIF-1α. *Cancer Res* **71:** 2260–2275. doi:10.1158/0008-5472.CAN-10-3007

Krizova J, Hulkova M, Capek V, Mlejnek P, Silhavy J, Tesarova M, Zeman J, Hansikova H. 2021. Microarray and qPCR analysis of mitochondrial metabolism activation during prenatal and early postnatal development in rats and humans with emphasis on CoQ_{10} biosynthesis. *Biology (Basel)* **10:** 418. doi:10.3390/biology10050418

Kukat C, Davies KM, Wurm CA, Spåhr H, Bonekamp NA, Kühl I, Joos F, Polosa PL, Park CB, Posse V, et al. 2015. Cross-strand binding of TFAM to a single mtDNA molecule forms the mitochondrial nucleoid. *Proc Natl Acad Sci* **112:** 11288–11293. doi:10.1073/pnas.1512131112

LaGory EL, Wu C, Taniguchi CM, Ding CC, Chi JT, von Eyben R, Scott DA, Richardson AD, Giaccia AJ. 2015. Suppression of PGC-1alpha is critical for reprogramming oxidative metabolism in renal cell carcinoma. *Cell Rep* **12:** 116–127. doi:10.1016/j.celrep.2015.06.006

Lai L, Leone TC, Zechner C, Schaeffer PJ, Kelly SM, Flanagan DP, Medeiros DM, Kovacs A, Kelly DP. 2008. Transcriptional coactivators PGC-1alpha and PGC-lbeta control overlapping programs required for perinatal maturation of the heart. *Genes Dev* **22:** 1948–1961. doi:10.1101/gad.1661708

Lambertini E, Penolazzi L, Morganti C, Lisignoli G, Zini N, Angelozzi M, Bonora M, Ferroni L, Pinton P, Zavan B. 2015. Osteogenic differentiation of human MSCs: specific occupancy of the mitochondrial DNA by NFATc1 transcription factor. *Int J Biochem Cell Biol* **64:** 212–219. doi:10.1016/j.biocel.2015.04.011

Larsson NG, Wang J, Wilhelmsson H, Oldfors A, Rustin P, Lewandoski M, Barsh GS, Clayton DA. 1998. Mitochondrial transcription factor A is necessary for mtDNA maintenance and embryogenesis in mice. *Nat Genet* **18:** 231–236. doi:10.1038/ng0398-231

Latour MA, Peebles ED, Boyle CR, Brake JD, Kellogg TF. 1995. Changes in serum lipid, lipoprotein and corticosterone concentrations during neonatal chick development. *Biol Neonate* **67:** 381–386. doi:10.1159/000244189

Leveille GA. 1969. In vitro hepatic lipogenesis in the hen and chick. *Comp Biochem Physiol* **28:** 431–435. doi:10.1016/0010-406X(69)91357-7

Levin M, Anavy L, Cole AG, Winter E, Mostov N, Khair S, Senderovich N, Kovalev E, Silver DH, Feder M, et al. 2016. The mid-developmental transition and the evolution of animal body plans. *Nature* **531:** 637–641. doi:10.1038/nature16994

Li H, Durbin R. 2009. Fast and accurate short read alignment with Burrows–Wheeler transform. *Bioinformatics* **25:** 1754–1760. doi:10.1093/bioinformatics/btp324

Love MI, Huber W, Anders S. 2014. Moderated estimation of fold change and dispersion for RNA-seq data with DESeq2. *Genome Biol* **15:** 550. doi:10.1186/s13059-014-0550-8

Marin R, Cortez D, Lamanna F, Pradeepa MM, Leushkin E, Julien P, Liechti A, Halbert J, Bruning T, Mössinger K, et al. 2017. Convergent origination of a *Drosophila*-like dosage compensation mechanism in a reptile lineage. *Genome Res* **27:** 1974–1987. doi:10.1101/gr.223727.117

Matkovich SJ, Edwards JR, Grossenheider TC, de Guzman Strong C, Dorn GW 2nd. 2014. Epigenetic coordination of embryonic heart

transcription by dynamically regulated long noncoding RNAs. *Proc Natl Acad Sci* **111:** 12264–12269. doi:10.1073/pnas.1410622111
McShane E, Couvillion M, Ietswaart R, Prakash G, Smalec BM, Soto I, Baxter-Koenigs AR, Choquet K, Churchman LS. 2024. A kinetic dichotomy between mitochondrial and nuclear gene expression processes. *Mol Cell* **84:** 1541–1555.e11. doi:10.1016/j.molcel.2024.02.028
Medini H, Cohen T, Mishmar D. 2020. Mitochondria are fundamental for the emergence of metazoans: on metabolism, genomic regulation, and the birth of complex organisms. *Annu Rev Genet* **54:** 151–166. doi:10.1146/annurev-genet-021920-105545
Medini H, Cohen T, Mishmar D. 2021a. Mitochondrial gene expression in single cells shape pancreatic beta cells' sub-populations and explain variation in insulin pathway. *Sci Rep* **11:** 466. doi:10.1038/s41598-020-80334-w
Medini H, Zirman A, Mishmar D. 2021b. Immune system cells from COVID-19 patients display compromised mitochondrial-nuclear expression co-regulation and rewiring toward glycolysis. *iScience* **24:** 103471. doi:10.1016/j.isci.2021.103471
Meiklejohn CD, Holmbeck MA, Siddiq MA, Abt DN, Rand DM, Montooth KL. 2013. An incompatibility between a mitochondrial tRNA and its nuclear-encoded tRNA synthetase compromises development and fitness in *Drosophila*. *PLoS Genet* **9:** e1003238. doi:10.1371/journal.pgen.1003238
Minai L, Martinovic J, Chretien D, Dumez F, Razavi F, Munnich A, Rötig A. 2008. Mitochondrial respiratory chain complex assembly and function during human fetal development. *Mol Genet Metab* **94:** 120–126. doi:10.1016/j.ymgme.2007.12.007
Mishmar D, Ruiz-Pesini E, Brandon M, Wallace DC. 2004. Mitochondrial DNA-like sequences in the nucleus (NUMTs): insights into our African origins and the mechanism of foreign DNA integration. *Hum Mutat* **23:** 125–133. doi:10.1002/humu.10304
Mitros T, Lyons JB, Session AM, Jenkins J, Shu S, Kwon T, Lane M, Ng C, Grammer TC, Khokha MK, et al. 2019. A chromosome-scale genome assembly and dense genetic map for *Xenopus tropicalis*. *Dev Biol* **452:** 8–20. doi:10.1016/j.ydbio.2019.03.015
Moran BM, Payne CY, Powell DL, Iverson EN, Donny AE, Banerjee SM, Langdon QK, Gunn TR, Rodriguez-Soto RA, Madero A. 2024. A lethal mitonuclear incompatibility in complex I of natural hybrids. *Nature* **626:** 119–127. doi:10.1038/s41586-023-06895-8
Nakada Y, Canseco DC, Thet S, Abdisalaam S, Asaithamby A, Santos CX, Shah AM, Zhang H, Faber JE, Kinter MT, et al. 2017. Hypoxia induces heart regeneration in adult mice. *Nature* **541:** 222–227. doi:10.1038/nature20173
Nandi S, Liang G, Sindhava V, Angireddy R, Basu A, Banerjee S, Hodawadekar S, Zhang Y, Avadhani NG, Sen R. 2020. YY1 control of mitochondrial-related genes does not account for regulation of immunoglobulin class switch recombination in mice. *Eur J Immunol* **50:** 822–838. doi:10.1002/eji.201948385
Noble RC, Cocchi M. 1990. Lipid metabolism and the neonatal chicken. *Prog Lipid Res* **29:** 107–140. doi:10.1016/0163-7827(90)90014-C
Papier O, Minor G, Medini H, Mishmar D. 2022. Coordination of mitochondrial and nuclear gene-expression regulation in health, evolution, and disease. *Curr Opin Physiol* **27:** 100554. doi:10.1016/j.cophys.2022.100554
Pejznochova M, Tesarova M, Hansikova H, Magner M, Honzik T, Vinsova K, Hajkova Z, Havlickova V, Zeman J. 2010. Mitochondrial DNA content and expression of genes involved in mtDNA transcription, regulation and maintenance during human fetal development. *Mitochondrion* **10:** 321–329. doi:10.1016/j.mito.2010.01.006
Popov LD. 2020. Mitochondrial biogenesis: an update. *J Cell Mol Med* **24:** 4892–4899. doi:10.1111/jcmm.15194
Porporato PE, Dhup S, Dadhich RK, Copetti T, Sonveaux P. 2011. Anticancer targets in the glycolytic metabolism of tumors: a comprehensive review. *Front Pharmacol* **2:** 49. doi:10.3389/fphar.2011.00049
Puigserver P, Wu Z, Park CW, Graves R, Wright M, Spiegelman BM. 1998. A cold-inducible coactivator of nuclear receptors linked to adaptive thermogenesis. *Cell* **92:** 829–839. doi:10.1016/S0092-8674(00)81410-5
R Core Team. 2013. *R: a language and environment for statistical computing*. R Foundation for Statistical Computing, Vienna. https://www.R-project.org/.
Read JA, Winter VJ, Eszes CM, Sessions RB, Brady RL. 2001. Structural basis for altered activity of M- and H-isozyme forms of human lactate dehydrogenase. *Proteins* **43:** 175–185. doi:10.1002/1097-0134(20010501)43:2<175::AID-PROT1029>3.0.CO;2-#
Reznik E, Wang Q, La K, Schultz N, Sander C. 2017. Mitochondrial respiratory gene expression is suppressed in many cancers. *eLife* **6:** e21592. doi:10.7554/eLife.21592
Sanger TJ, Losos JB, Gibson-Brown JJ. 2008. A developmental staging series for the lizard genus Anolis: a new system for the integration of evolution, development, and ecology. *J Morphol* **269:** 129–137. doi:10.1002/jmor.10563
Scarpulla RC. 2002. Nuclear activators and coactivators in mammalian mitochondrial biogenesis. *Biochim Biophys Acta* **1576:** 1–14. doi:10.1016/S0167-4781(02)00343-3
Secco I, Giacca M. 2023. Regulation of endogenous cardiomyocyte proliferation: the known unknowns. *J Mol Cell Cardiol* **179:** 80–89. doi:10.1016/j.yjmcc.2023.04.001
Shao D, Liu Y, Liu X, Zhu L, Cui Y, Cui A, Qiao A, Kong X, Liu Y, Chen Q. 2010. PGC-1β-Regulated mitochondrial biogenesis and function in myotubes is mediated by NRF-1 and ERRα. *Mitochondrion* **10:** 516–527. doi:10.1016/j.mito.2010.05.012
Sharma A, Ford S, Calvert J. 2014. Adaptation for life: a review of neonatal physiology. *Anaesth Intensive Care Med* **15:** 89–95. doi:10.1016/j.mpaic.2014.01.002
She H, Yang Q, Shepherd K, Smith Y, Miller G, Testa C, Mao Z. 2011. Direct regulation of complex I by mitochondrial MEF2D is disrupted in a mouse model of Parkinson disease and in human patients. *J Clin Invest* **121:** 930–940. doi:10.1172/JCI43871
Singh A, Happel C, Manna SK, Acquaah-Mensah G, Carrerero J, Kumar S, Nasipuri P, Krausz KW, Wakabayashi N, Dewi R, et al. 2013. Transcription factor NRF2 regulates miR-1 and miR-206 to drive tumorigenesis. *J Clin Invest* **123:** 2921–2934. doi:10.1172/JCI66353
Takagi H, Tamura I, Fujimura T, Doi-Tanaka Y, Shirafuta Y, Mihara Y, Maekawa R, Taketani T, Sato S, Tamura H, et al. 2022. Transcriptional coactivator PGC-1alpha contributes to decidualization by forming a histone-modifying complex with C/EBPbeta and p300. *J Biol Chem* **298:** 101874. doi:10.1016/j.jbc.2022.101874
Talman V, Teppo J, Poho P, Movahedi P, Vaikkinen A, Karhu ST, Trost K, Suvitaival T, Heikkonen J, Pahikkala T, et al. 2018. Molecular atlas of postnatal mouse heart development. *J Am Heart Assoc* **7:** e010378. doi:10.1161/JAHA.118.010378
Tavares CDJ, Aigner S, Sharabi K, Sathe S, Mutlu B, Yeo GW, Puigserver P. 2020. Transcriptome-wide analysis of PGC-1alpha-binding RNAs identifies genes linked to glucagon metabolic action. *Proc Natl Acad Sci* **117:** 22204–22213. doi:10.1073/pnas.2000643117
Ticci C, Orsucci D, Ardissone A, Bello L, Bertini E, Bonato I, Bruno C, Carelli V, Diodato D, Doccini S, et al. 2021. Movement disorders in children with a mitochondrial disease: a cross-sectional survey from the nationwide Italian collaborative network of mitochondrial diseases. *J Clin Med* **10:** 2063. doi:10.3390/jcm10102063
Tranchant C, Anheim M. 2016. Movement disorders in mitochondrial diseases. *Rev Neurol (Paris)* **172:** 524–529. doi:10.1016/j.neurol.2016.07.003
van Waveren C, Moraes CT. 2008. Transcriptional co-expression and co-regulation of genes coding for components of the oxidative phosphorylation system. *BMC Genomics* **9:** 18. doi:10.1186/1471-2164-9-18
Webster WS, Abela D. 2007. The effect of hypoxia in development. *Birth Defects Res C Embryo Today* **81:** 215–228. doi:10.1002/bdrc.20102
Wellen KE, Thompson CB. 2012. A two-way street: reciprocal regulation of metabolism and signalling. *Nat Rev Mol Cell Biol* **13:** 270–276. doi:10.1038/nrm3305
Wickham H. 2016. *ggplot2: elegant graphics for data analysis*. Springer-Verlag, New York.
Wolf AR, Mootha VK. 2014. Functional genomic analysis of human mitochondrial RNA processing. *Cell Rep* **7:** 918–931. doi:10.1016/j.celrep.2014.03.035
Wu Z, Puigserver P, Andersson U, Zhang C, Adelmant G, Mootha V, Troy A, Cinti S, Lowell B, Scarpulla RC, et al. 1999. Mechanisms controlling mitochondrial biogenesis and respiration through the thermogenic coactivator PGC-1. *Cell* **98:** 115–124. doi:10.1016/S0092-8674(00)80611-X
Xu E, Zhang L, Yang H, Shen L, Feng Y, Ren M, Xiao Y. 2019. Transcriptome profiling of the liver among the prenatal and postnatal stages in chickens. *Poult Sci* **98:** 7030–7040. doi:10.3382/ps/pez434
Zhang Z. 2016. Reshaping and aggregating data: an introduction to reshape package. *Ann Transl Med* **4:** 78. doi:10.3978/j.issn.2305-5839.2016.01.33
Zhao Q, Sun Q, Zhou L, Liu K, Jiao K. 2019. Complex regulation of mitochondrial function during cardiac development. *J Am Heart Assoc* **8:** e012731. doi:10.1161/JAHA.119.012731

Received June 25, 2024; accepted in revised form February 4, 2025.